

Hydraulic Investigations of the Erosion Potential of Flows Overtopping Owyhee Dam - Owyhee Project, Oregon-Idaho Pacific Northwest Region

Sensitive Information – For Official Use Only

July 2006

Kathleen H. Frizell

Hydraulic Engineer
US Bureau of Reclamation
Technical Services Center
Water Resources Research Laboratory
Denver, Colorado

Executive Summary

This report describes the investigation into the location and erosive power of the jet impingement on the rock abutments during the potential overtopping of Owyhee Dam. The investigation used the latest technology available to define the jet trajectory and the impact zone and determined the energy available at various impact elevations. Information is provided so that a decision may be made regarding whether or not the dam abutments are adequate to ensure stability of the right abutment gravity dam, the spillway tunnel through the right abutment, and the thick-arch concrete dam. Further study may be required if it is determined that the results presented indicate unacceptable risk for the dam.

The Owyhee project is located in southeastern Oregon approximately 50 miles west of Boise Idaho and about 24 miles south of Vale, Oregon. Owyhee Dam stores 1.12 million acre-feet of water for irrigation of project lands and is the key feature of the project, figure 1. The project also provides recreation, and fish and wildlife benefits. The drainage basin has an area of 10,900 square miles.

The dam has a thick-arch concrete dam section 623 feet long and a concrete gravity section 210 feet long located on the right abutment. Top of dam is at El. 2675 with the top of the parapet wall at El. 2678.67. The morning glory spillway inlet crest is at elevation 2658 and is about 52 feet in diameter. Below the morning glory shape the vertical shaft tapers from a diameter of 31.92 feet at elevation 2637.26 to 22.6 feet at elevation 2513, 145 feet below the crest. The spillway has a capacity of 41,789 ft³/s at elevation 2675, which is the top of the dam. Construction of the dam began in 1928 and was completed in 1932.

The flood routings recently developed for Owyhee Dam [3] are summarized in this document and were used in evaluation of the overtopping events.

The jet trajectories for overtopping events with flood frequencies of 5,000, 10,000, 20,000, 50,000, 100,000, 1,000,000, and 10,000,000 years were analyzed both through the air and in the tailwater pool. The results of the jet trajectories are plotted on figure 10. The results of the analysis for the PMF are summarized in table 5. The footprint of the jet from the PMF is shown on figure 9 in the body of the report. The tailwater for the PMF is at El. 2531. The footprint of the jet impinges on both the right and left abutment areas above the tailwater.

The plot of the relationship between the erodibility index and the stream power indicates that erosion would be expected in the rock abutment areas throughout the rock layers under the PMF. The stream power density is computed based upon the determination of the jet characteristics both above and below the tailwater. The stream power is a function of the area of the jet that impinges on the various surfaces at the various locations. Figure 12 shows the plot of the stream power and erodibility for evaluation of the PMF event.

The PMF stream power at the impingement locations on the abutments and into the tailwater is between 81 and 432 HP/ft² (647 and 3467 kW/m²), respectively. The stream power is a maximum of 647 HP/ft² (3467 kW/m²) for the free-falling jet at El. 2531 where the jet would impact the tailwater. In the tailwater, the core of the jet is fully dissipated after plunging 10 ft or at El. 2521. The outer edge of the jet spreads and continues through the pool increasing the footprint or area of the jet, thus decreasing the power per square foot in the pool.

The following recommendations are made based on the findings of these investigations for the PMF flow:

- Investigate whether the right abutment gravity section would remain stable with loss of a significant quantity of rock if erosion during overtopping were to occur.
- Investigate whether the rock cover over the spillway tunnel would remain adequate if some rock erodes above the tunnel.
- Determine if there is another flood event with a higher probability of occurrence that might have acceptable risk but potentially less probability for abutment erosion. Plots of the erodibility index and stream power for various flood frequencies are provided in the appendix.

There is still quite a bit of uncertainty in the analysis of the jet characteristics. Most of the research has been based upon model results, some of which had significant scale effects. In addition, the majority of the work was conducted for circular jets from nozzles, from which area conversions have been made for the rectangular jet formed during an overtopping event. This greatly increases the uncertainty in the results

presented. As such, conservative judgment has been used as much as possible throughout the investigation. The rock erodibility is also based upon estimates of the rock quality from a limited number of drill holes. The process utilized by Annandale [8] emphasizes the RQD factor more than joint orientation, etc. and this has led to necessary judgments in the rock erodibility that will also lead to uncertainty in the results. More research is needed to increase the reliability of the conclusions presented.

Introduction

These investigations were requested by John Baals, Manager, Structural Analysis Group, 86-68110, to assist with the Comprehensive Facility Review (CFR) for Owyhee Dam. Several potential failure modes were identified in the CFR for Owyhee Dam. Failure modes based on foundation erosion weren't a concern in the past because the overtopping flows previously predicted weren't considered to be large. Results from later flood hazard analyses showed significant overtopping would occur under the revised Probable Maximum Flood (PMF). Geotechnical Engineering experts within Reclamation thought that there could be sufficient energy to cause erosion that could either compromise the gravity or arch dam foundation or erode rock cover from the spillway tunnel that is required for stability.

Evaluation of the failure modes provides a tool for a better understanding of the performance and risks at Owyhee Dam and for focusing the monitoring program to ensure that conditions remain as expected, or any changes in behavior are promptly observed and reported so that the appropriate responses can be taken to prevent failure.

This report documents the analyses performed to address the potential failure mode identified as foundation instability or loss of cover over spillway tunnel from erosion of the dam abutments during PMF overtopping. In addition, other flood events with lesser frequency were also investigated. These hydraulic analyses, considering the erodibility of the rock material, will attempt to provide information to assess these failure modes.

Purpose

The purpose of this report is to document the results of the hydraulic investigations regarding overtopping of the dam and impingement of the jet and the subsequent hydraulic loading on the dam rock abutments for Owyhee Dam, Oregon. The investigations were based on the 2005 flood analysis and knowledge of the existing abutment rock materials.

Background

The Owyhee project is located in southeastern Oregon approximately 50 miles west of Boise Idaho and about 24 miles south of Vale, Oregon. Owyhee Dam stores 1.12 million acre-feet of water for irrigation of project lands and is the key feature of the project, figure 1. The project also provides recreation, and fish and wildlife benefits. The drainage basin has an area of 10,900 square miles.

The dam has a thick-arch concrete dam section 623 feet long and a concrete gravity section 210 feet long located on the right abutment. Construction of the dam began in 1928 and was completed in 1932.

The morning glory spillway inlet crest is at elevation 2658 and is about 52 feet in diameter.

Below the morning glory shape the vertical shaft tapers from a diameter of 31.92 feet at elevation 2637.26 to 22.6 feet at elevation 2513, 145 feet below the crest. A radius elbow section connects the shaft and tunnel. The entire shaft and elbow section at the base of the shaft are lined with concrete, assumed to be unreinforced. The spillway tunnel is a circular section 22.6 feet in diameter. The concrete tunnel lining is reinforced for 50 feet downstream of the elbow, to station 5+00, and for 50 feet at the outlet between stations 11+00 and 11+50. The remainder of the tunnel between stations 5+00 and 11+00 is lined with unreinforced concrete. The minimum concrete lining thickness for the elbow and the reach 300 feet downstream of the inlet (to Station 7+00) is 21 inches. From Station 7+00 downstream the minimum lining thickness is 12 inches. The spillway has a capacity of 41,789 ft³/s at elevation 2675, which is the top of the dam.

The outlet works consist of three conduits through the dam controlled by 3-40-inch jet flow gates at the downstream end. The capacity of the outlet works is 2800 ft³/s at elevation 2670.

A plan view and section of the dam, spillway alignment, and outlet works location is shown on figures 2 and 3.

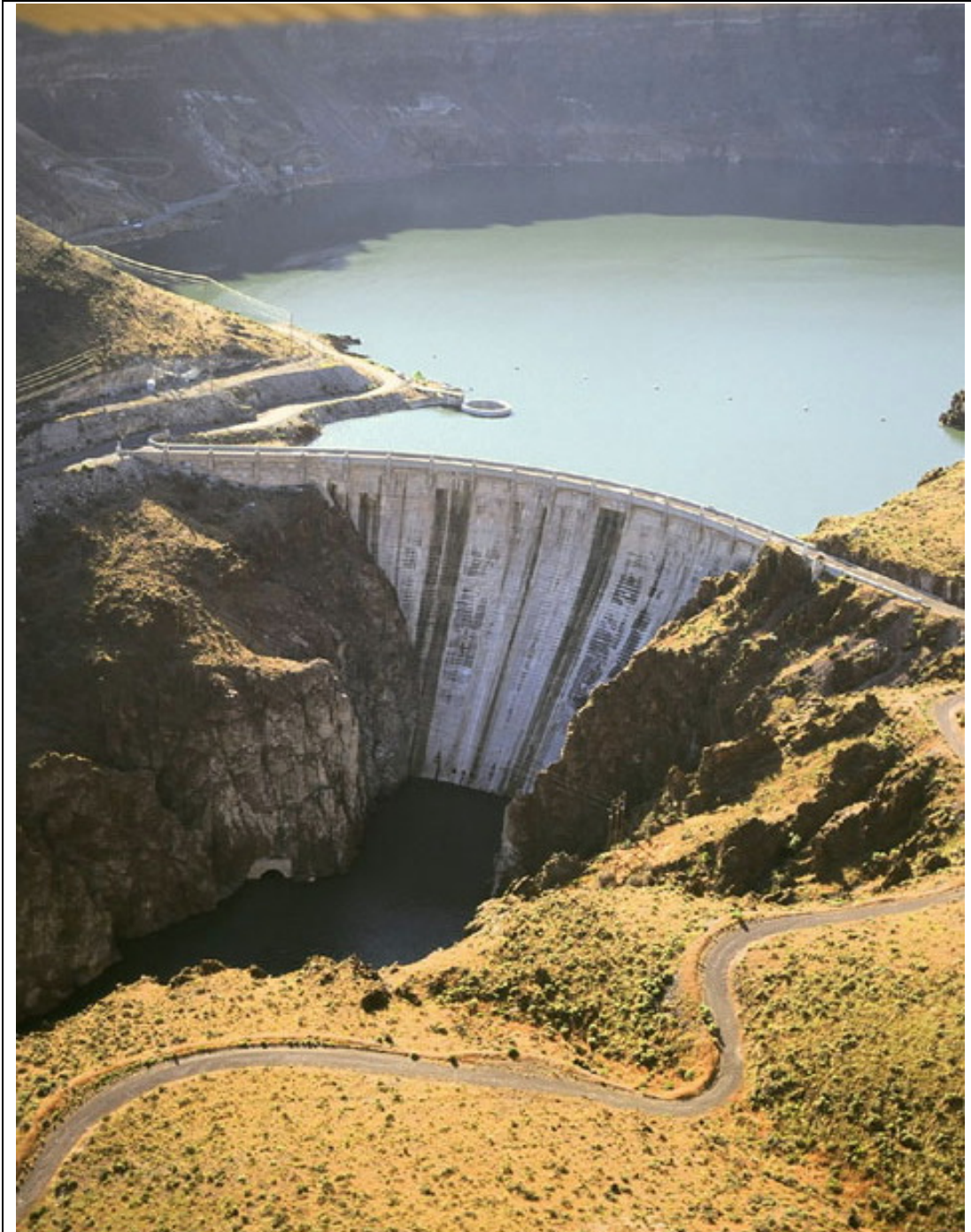


Figure 1. - Aerial view of Owyhee Dam. (Reclamation photo by Dave Walsh, June 22, 2005.)

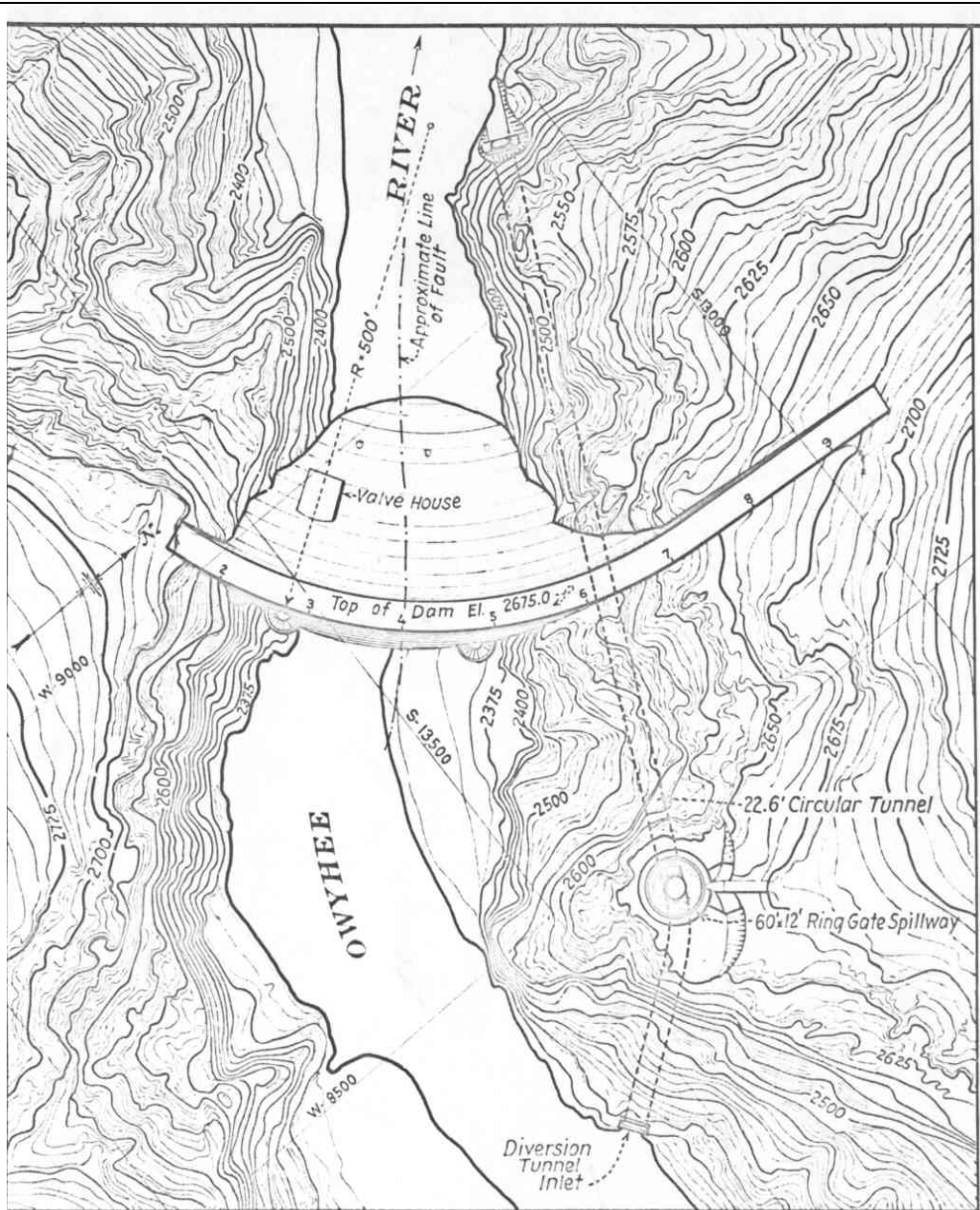


Figure 2. - Plan view of Owyhee Dam showing the dam, the morning-glory spillway near the right abutment, and the outlet works on the left side of the river channel. (This is a portion of drawing 48-D-69.)

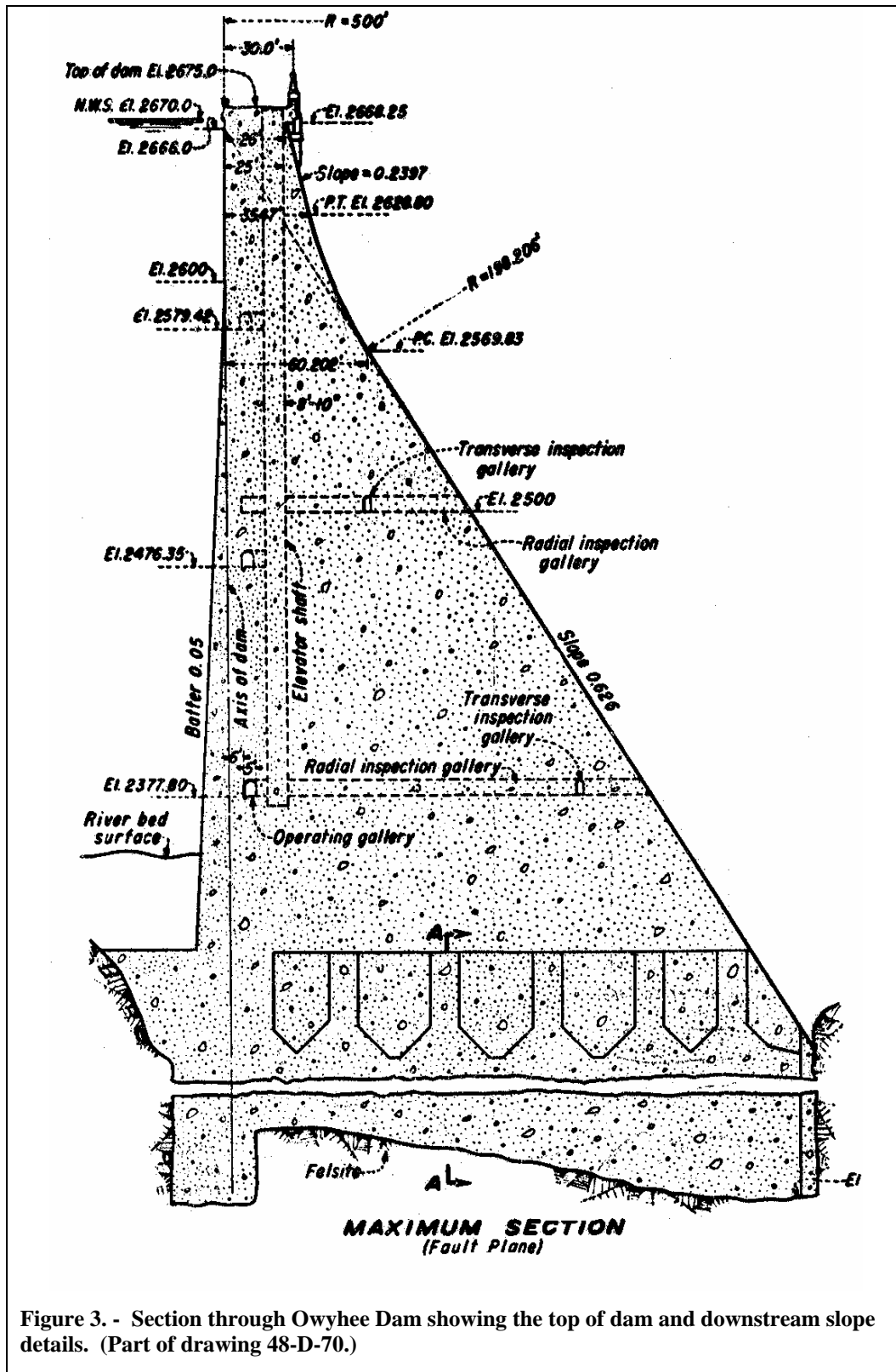


Figure 3. - Section through Owyhee Dam showing the top of dam and downstream slope details. (Part of drawing 48-D-70.)

Site Geology

The dam, spillway, and other appurtenances are located in the Owyhee uplands and founded on a Tertiary rhyolitic volcanic sequence composed primarily of rhyolite (Tr) with associated flow lithologies consisting of pitchstone (Tpm) and pitchstone agglomerate (Tpa) with co-eruptive tuff (Tt).

Several geologic investigations have taken place since construction of the dam. In 1981, a geologic mapping program was conducted as part of the Safety Evaluation of Existing Dams program. Topographic and surficial geologic mapping, delineation of seepage areas and fault zones, and a discontinuity survey at the site was completed [1].

The most recent geologic investigations were done in 1991 [2]. There was one drill hole on each abutment through the concrete and into the foundation. Drill hole DH-90-1 on the left abutment at station 1+22 went through 1.5 feet of concrete to a depth of 150 feet. Drill hole DH-90-2 on the right abutment at station 8+13 went through 36.7 feet of concrete to a depth of 150 feet.

The site geology was used in determination of the erodibility index of the abutments for evaluating the potential for erosion during the PMF overtopping as discussed in a following section.

Flood Routings

Flood routings performed for Owyhee Dam are documented in Technical Memorandum (TM) OWY-8130-CFR-2006-1 [3]. The TM documented the results of various studies and determined data such as maximum reservoir water surface (RWS) elevations, freeboard values, overtopping depths, durations, and peak outflows for the general storm rain-on-snow flood frequency hydrographs.

Flood routings were performed for the rain on snow events and for initial starting reservoir water surface elevations of 2373, 2644, 2659, and top of active storage at 2670. The parapet wall at El. 2678.67 was assumed to remain intact during the flood and was used as the overtopping elevation with a dam crest length of 810 ft during the routings. Table 1 shows the flood routing results developed for top of active storage as the initial condition. This initial was surface elevation was chosen to produce a conservative or maximum overtopping condition for the following hydraulic and erodibility analysis.

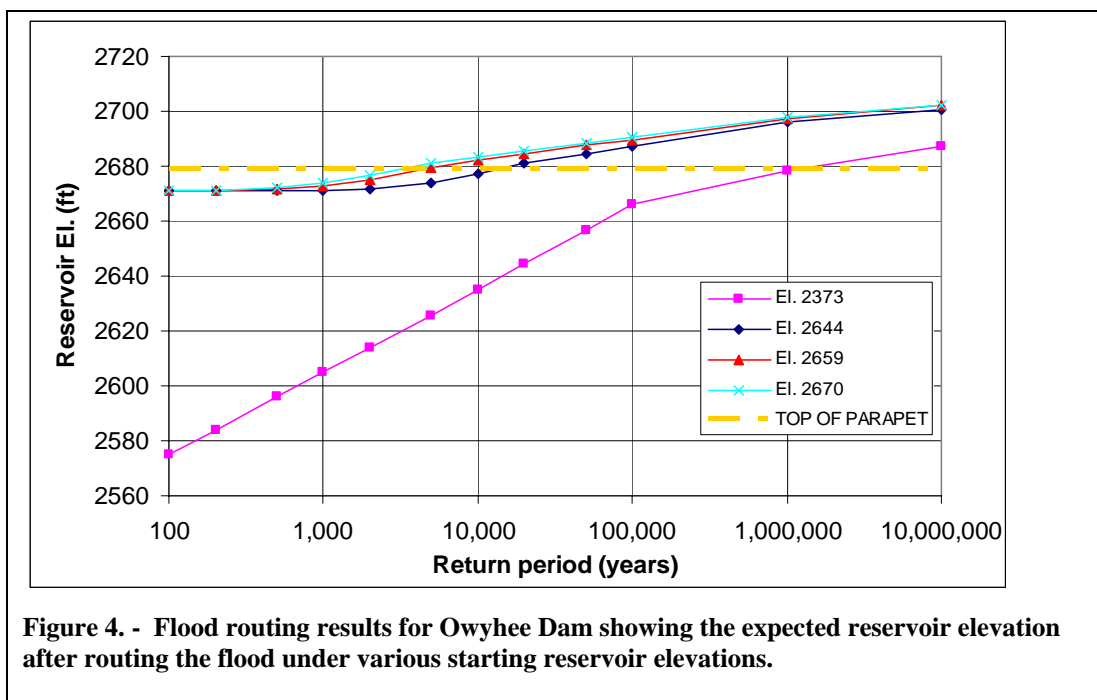
Figures 4 and 5 shows the relationship between the flood routings for the various starting reservoir elevations. Based upon top of parapet El. 2678.67, figure 3 shows that overtopping is expected to initiate at a return period of about 4,000 years with top of active as the initial routing reservoir elevation. As the beginning elevation for the routing decreases the return period frequency increases before overtopping will begin, but overtopping will occur at the 1,000,000-year event even with starting RWS of 2373.

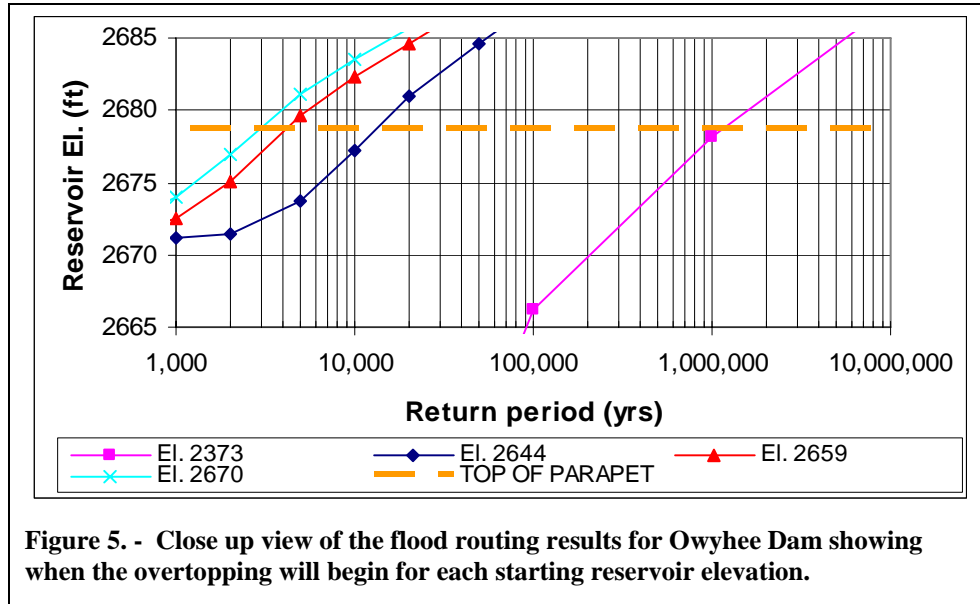
Table 1. –Flood routing results with starting reservoir water surface of 2670 ft.

Flood (years)	Peak Inflow (ft ³ /s)	Volume (acre- feet)	Max. RWS (feet)	Peak Discharge (ft ³ /s)		Freeboard (feet) ¹	Overtopping	
				Spillway	Top of Dam		Start (hour)	Duration (hours)
100	35,059	401,171	2,671.19	32,829	0	7.48	N/A	N/A
200	43,527	446,620	2,671.33	37,823	0	7.34	N/A	N/A
500	56,576	514,452	2,672.22	40,828	0	6.45	N/A	N/A
1000	68,000	572,333	2,674.06	41,710	0	4.61	N/A	N/A
2000	80,900	636,508	2,676.93	41,916	0	1.74	N/A	N/A
5000	100,450	732,042	2,681.13	41,594	8,208	-2.46	156	63
10,00	117,314	813,246	2,683.47	41,179	22,286	-4.80	147	86
20,000	136,138	902,920	2,685.61	40,794	38,765	-6.94	143	98
50,000	164,315	1,035,746	2,688.36	40,292	64,052	-9.69	139	110
100,000	188,353	1,148,069	2,690.48	39,903	86,128	-11.81	137	117
1,000,000	287,744	1,606,636	2,697.95	38,496	179,656	-19.28	131	133
10,000,000	356,000	1,918,399	2,702.42	37,629	245,662	-23.75	129	139

¹ Negative values indicate overtopping of the dam parapet walls.

The maximum overtopping depth is 23.75 feet with a discharge of 245,662 ft³/s under reservoir El. 2702.42 for the 10,000,000-year PMF condition. The maximum duration of overtopping for the PMF is approximately 139 hours. This duration is considered long enough to present a significant hydrodynamic loading on the downstream abutments due to impinging flows on the abutment surfaces above the tailwater. These routing results were used to evaluate the overtopping trajectories and potential for hydrodynamic loading on the downstream abutments.





Tailwater Information

Information regarding the tailwater expected at the toe of the dam was obtained for the various flood frequencies identified in table 1 to allow determination of the flow characteristics through the tailwater and the effect of tailwater on hydrodynamic loading. Bruce Fienberg, 86-68540, performed a very preliminary estimate of the tailwater at the toe of Owyhee Dam using a MIKE11 - 1D model. Overtopping with no breach of the dam was assumed. The modeling used cross sections developed from the USGS 10-meter, level 2 digital elevation models of terrain data. A bottom elevation of 2358 was used for the cross section at the toe of the dam. The outflow hydrograph from the flood routing [3] was used as an inflow boundary condition to the MIKE11 model. The top of the parapet at El. 2678.67 with a dam crest length of 833 ft was used for the top of dam crest. This allowed for a simulation of the drop that takes place between the dam crest and the downstream channel at the toe of the dam. The Manning's roughness for the downstream channel was assumed to be 0.045.

Table 2 and figure 6 show the results of the MIKE11 modeling for the tailwater at the toe of Owyhee Dam [4]. The uncertainty in these tailwater elevation predictions was not quantitatively evaluated. The maximum elevation near the toe of the dam is El. 2531 ft under the PMF. The tailwater may be affected by the dynamics of the flow over the top of the dam, thus producing slightly different results. In addition, if tailwater elevation ends up playing a significant role in the outcome of the hydrodynamic loading, then a more detailed modeling effort should be undertaken. The following sections will determine the characteristics of the jet and potential for erosion above and below the tailwater.

Table 2. - Tailwater results for the toe of Owyhee Dam based upon MIKE11 modeling.

Return period (yrs)	Total outflow (ft ³ /s)	Tailwater at toe of dam (ft)
100	32,829	2428

Return period (yrs)	Total outflow (ft ³ /s)	Tailwater at toe of dam (ft)
200	37,823	2433
500	40,828	2435
1,000	41,710	2436
2,000	41,916	2436
5,000	49,802	2443
10,000	63,465	2451
20,000	79,559	2461
50,000	104,344	2473
100,000	126,031	2482
1,000,000	218,152	2514
10,000,000	283,291	2531

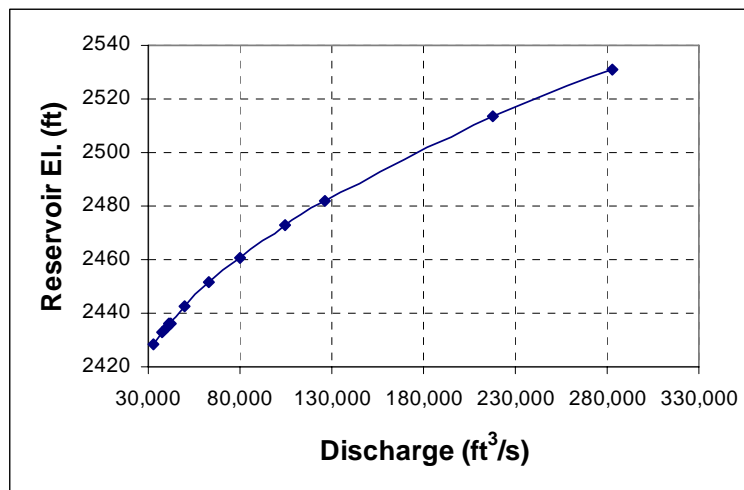


Figure 6. - Estimated tailwater curve for the toe of Owyhee Dam.

Hydrodynamic Loading

Reservoir flows over the top of a concrete dam can erode the foundation and the concrete at the toe of the dam and along the abutments. The amount of erosion depends on the duration of flow, the amount of flow, the height of drop of the overflowing jet of water, the depth of tailwater, and the erodibility of the foundation.

The focus of this document is to determine the hydraulic loading associated with overtopping under the PMF from the June 2006 flood routing [3]. In addition, the jet trajectories for other flood return periods were also computed and are located in the appendix. The loading is not concerned with the spillway or outlet works flows but only the amount of water going over the top of the dam parapet walls. Several aspects of the overtopping need to be addressed:

1. The jet characteristics including the jet trajectory and impingement location, and spread of the jet, both above and below the tailwater.
2. Computation of the stream power associated with the jet.

3. Evaluation of the erodibility of the rock abutment material based upon the computed stream power and estimated erodibility factors for the rock.

The following are the necessary parameters:

- $Q_{\text{overtop}} = 245,662 \text{ ft}^3/\text{s}$, total duration of overtopping = 139 hours
- Parapet wall El. 2678.67 ft
- Top of dam El. 2675 ft
- Base of dam approximately El. 2358 ft
- Width of dam crest $W=30$ ft
- RWS El. 2702.42 with a depth of overtopping above the parapet walls under the PMF = 23.75 ft.
- Dam crest length $L = 810$ ft on a 500-ft radius at the upstream vertical dam face. Assume the flow will spring free from the parapet wall and be adequately aerated.
- Tailwater in the river at the toe of the dam is about El. 2531 ft under the PMF.

Definitions

The schematic in figure 7 shows various flow release situations or possibilities from dams with definition of the important parameters of a free falling jet into a plunge pool or potentially impacting a surface above the plunge pool shown in 7c [7].

D_i = diameter of the jet at issuance from the dam

D_j = jet thickness at impact with the plunge pool or on a surface

D_{out} = outer dimension of the jet including the inner core of the jet and the jet spread

t_i = jet thickness or overtopping depth at issuance from the dam

t_j = jet thickness at impact with the plunge pool or on a surface

$H = H_{\text{overtop}}$ = total head above the opening or over the crest

V_i = mean jet velocity at issuance from the dam

V_j = mean jet velocity at impact with the plunge pool or on a surface

Y = total plunge pool depth

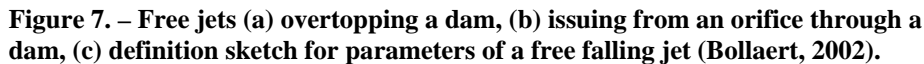
Z = difference between upstream and downstream water levels

θ_i = jet angle from horizontal at issuance from the dam

δ_{out} = angle of the outer jet spread in a free falling jet

α_{out} = angle of the outer jet spread in the plunge pool

Determination of the jet characteristics is the first step in estimating the erosion or scour potential of the rock. The flow will come over the top of the dam for the Owyhee Dam PMF event and will match the definition given as figure 7a.



Trajectory Calculations

The flow over the top of the dam and the free fall of the jet at the various elevations associated with impingement on the rock abutments and into the tailwater must be characterized. The jet trajectory is computed for the free fall where initial depth and velocity, initial turbulence, and fall length play a role. If there is adequate free fall the jet will begin aerating and spreading. With additional free fall the core of the jet may also begin to break up and dissipate, thus greatly

reducing impact on the rock surfaces. Once the free-falling jet enters the tailwater pool, the angle of entry and depth of the tailwater pool affects the jet spread and core diffusion of the jet. The following sections address the procedures used to determine the jet characteristics.

For Owyhee Dam overtopping, the initial angle of issuance is zero and the initial jet thickness or depth of overtopping is the brink depth with the parapet wall elevation 2678.67 as the datum. The brink depth and initial velocity are computed from the discharge over the dam. The critical flow depth is then computed by the relationship, $d_c = (q^2/g)^{1/3}$, where q is the discharge per unit of crest length [5]. The brink depth is then determined by the relationship developed between the critical and brink depth [6] and continuity. For the PMF overtopping of Owyhee Dam the unit discharge, $q = 303.29 \text{ ft}^3/\text{s}/\text{ft}$, the brink depth is equal to the initial depth of overtopping, $D_i = 10.15 \text{ ft}$, and the initial velocity at the brink is $V_i = 29.89 \text{ ft/s}$.

The flow over the top of the dam is simply a free overfall and is computed using the equation of motion assuming no aerodynamic influences on the jet [5]. The brink depth, velocity and velocity head are used for the computation of the jet trajectory.

The conventional form of the equation of projectile motion produces the following equation describing particle trajectory with the downstream edge of the parapet wall as the origin of an x-y coordinate system defining the bottom edge of the jet:

$$y = x \tan \theta_i - \frac{gx^2}{2V_i^2 \cos^2 \theta_i}$$

This equation is simplified when the jet issues horizontally from the top of the dam to:

$$y = -\frac{gx^2}{2V_i^2}$$

Further manipulation of the equation may be performed by replacing the initial velocity by the velocity head, $h_v = V_i^2/2g$ producing:

$$y = -\frac{x^2}{4h_v}$$

This equation approximates the lower free surface of the jet. The upper or outer edge of the jet is then defined by adding the initial depth or jet thickness to the bottom edge of the jet.

None of the above equations account for contraction and expansion of the jet prior to plunge into the tailwater pool or impingement on the rock. In the case of Owyhee Dam with free overflow over the dam, the horizontal travel and vertical drop of the jet to the point of impingement which will show the location of the impingement and determine the velocity of the jet to determine impingement forces, respectively.

Table 3 and figure 8 shows the result of the trajectory calculations for the Owyhee Dam under the PMF overtopping event. Figure 8 is a sectional view through the maximum dam section with the initial jet thickness shown as the brink depth. These results show the simple jet trajectory from the equation of motion. No spread of the outer diameter of the jet is shown, but will be computed in the following sections.

Figure 9 shows the predicted footprint of jet impingement on the rock abutments and into the tailwater pool at El. 2531. The plot was developed by radially offsetting the trajectory x and y distances to the intersection points with the contours or tailwater elevation. The concern is the pressure or force transmitted by the power of the jet as it impacts the surfaces above and below the tailwater.

The zone of impingement on the abutments above the tailwater is of concern both in the area beneath the dam gravity section and above the location of the spillway tunnel. From figure 9 it may be seen that the jet will impinge on the abutment in both these locations. The footprint is expanded close to the gravity section on the right abutment because of the short fall to that location and the thickness of the jet just after overtopping. The key is determining the power in the flow or pressure force exerted onto the surfaces by the flow impingement. The jet will then impact into the tailwater at the dam rock contact points and before impacting on the downstream face of the dam.

The core of the free-falling jet will, however, experience initial contraction, then potentially dissipation due to gravity with fall distance. As the jet enters the tailwater other factors combine to influence the decay of the core and spread or diffusion of the outer edges of the jet.

Table 3. - Free fall trajectory locations for the PMF event with x (horizontal) and y (vertical) distances and elevations from the downstream parapet location. Vertical fall continues as if unimpeded by abutments or tailwater.

select y	PMF			select y	PMF			select y	PMF			select y	PMF		
	x lower	el. Lower	el. Upper		x lower	el. Lower	el. Upper		x lower	el. Lower	el. Upper		x lower	el. Lower	el. Upper
0.00	0.00	2678.67	2688.82	-84.00	68.28	2594.67	2604.82	-166.00	95.99	2512.67	2522.82	-250.00	117.80	2428.67	2438.82
-2.00	10.54	2676.67	2686.82	-86.00	69.09	2592.67	2602.82	-168.00	96.57	2510.67	2520.82	-252.00	118.27	2426.67	2436.82
-4.00	14.90	2674.67	2684.82	-88.00	69.89	2590.67	2600.82	-170.00	97.14	2508.67	2518.82	-254.00	118.74	2424.67	2434.82
-6.00	18.25	2672.67	2682.82	-90.00	70.68	2588.67	2598.82	-172.00	97.71	2506.67	2516.82	-256.00	119.21	2422.67	2432.82
-8.00	21.07	2670.67	2680.82	-92.00	71.46	2586.67	2596.82	-174.00	98.28	2504.67	2514.82	-258.00	119.67	2420.67	2430.82
-10.00	23.56	2668.67	2678.82	-94.00	72.24	2584.67	2594.82	-176.00	98.84	2502.67	2512.82	-260.00	120.14	2418.67	2428.82
-12.00	25.81	2666.67	2676.82	-96.00	73.00	2582.67	2592.82	-178.00	99.40	2500.67	2510.82	-262.00	120.60	2416.67	2426.82
-14.00	27.88	2664.67	2674.82	-98.00	73.76	2580.67	2590.82	-180.00	99.96	2498.67	2508.82	-264.00	121.06	2414.67	2424.82
-16.00	29.80	2662.67	2672.82	-100.00	74.50	2578.67	2588.82	-182.00	100.51	2496.67	2506.82	-266.00	121.51	2412.67	2422.82
-18.00	31.61	2660.67	2670.82	-102.00	75.25	2576.67	2586.82	-184.00	101.06	2494.67	2504.82	-268.00	121.97	2410.67	2420.82
-20.00	33.32	2658.67	2668.82	-104.00	75.98	2574.67	2584.82	-186.00	101.61	2492.67	2502.82	-270.00	122.42	2408.67	2418.82
-22.00	34.95	2656.67	2666.82	-106.00	76.71	2572.67	2582.82	-188.00	102.16	2490.67	2500.82	-272.00	122.88	2406.67	2416.82
-24.00	36.50	2654.67	2664.82	-108.00	77.43	2570.67	2580.82	-190.00	102.70	2488.67	2498.82	-274.00	123.33	2404.67	2414.82
-26.00	37.99	2652.67	2662.82	-110.00	78.14	2568.67	2578.82	-192.00	103.24	2486.67	2496.82	-276.00	123.78	2402.67	2412.82
-28.00	39.42	2650.67	2660.82	-112.00	78.85	2566.67	2576.82	-194.00	103.77	2484.67	2494.82	-278.00	124.22	2400.67	2410.82
-30.00	40.81	2648.67	2658.82	-114.00	79.55	2564.67	2574.82	-196.00	104.31	2482.67	2492.82	-280.00	124.67	2398.67	2408.82
-32.00	42.15	2646.67	2656.82	-116.00	80.24	2562.67	2572.82	-198.00	104.84	2480.67	2490.82	-282.00	125.11	2396.67	2406.82
-34.00	43.44	2644.67	2654.82	-118.00	80.93	2560.67	2570.82	-200.00	105.37	2478.67	2488.82	-284.00	125.56	2394.67	2404.82
-36.00	44.70	2642.67	2652.82	-120.00	81.62	2558.67	2568.82	-202.00	105.89	2476.67	2486.82	-286.00	126.00	2392.67	2402.82
-38.00	45.93	2640.67	2650.82	-122.00	82.29	2556.67	2566.82	-204.00	106.41	2474.67	2484.82	-288.00	126.44	2390.67	2400.82
-40.00	47.12	2638.67	2648.82	-124.00	82.96	2554.67	2564.82	-206.00	106.93	2472.67	2482.82	-290.00	126.88	2388.67	2398.82
-42.00	48.28	2636.67	2646.82	-126.00	83.63	2552.67	2562.82	-208.00	107.45	2470.67	2480.82	-292.00	127.31	2386.67	2396.82
-44.00	49.42	2634.67	2644.82	-128.00	84.29	2550.67	2560.82	-210.00	107.97	2468.67	2478.82	-294.00	127.75	2384.67	2394.82
-46.00	50.53	2632.67	2642.82	-130.00	84.95	2548.67	2558.82	-212.00	108.48	2466.67	2476.82	-296.00	128.18	2382.67	2392.82
-48.00	51.62	2630.67	2640.82	-132.00	85.60	2546.67	2556.82	-214.00	108.99	2464.67	2474.82	-298.00	128.62	2380.67	2390.82
-50.00	52.68	2628.67	2638.82	-134.00	86.25	2544.67	2554.82	-216.00	109.50	2462.67	2472.82	-300.00	129.05	2378.67	2388.82
-52.00	53.73	2626.67	2636.82	-136.00	86.89	2542.67	2552.82	-218.00	110.00	2460.67	2470.82	-302.00	129.48	2376.67	2386.82
-54.00	54.75	2624.67	2634.82	-138.00	87.52	2540.67	2550.82	-220.00	110.51	2458.67	2468.82	-304.00	129.90	2374.67	2384.82
-56.00	55.75	2622.67	2632.82	-140.00	88.16	2538.67	2548.82	-222.00	111.01	2456.67	2466.82	-306.00	130.33	2372.67	2382.82
-58.00	56.74	2620.67	2630.82	-142.00	88.78	2536.67	2546.82	-224.00	111.51	2454.67	2464.82	-308.00	130.76	2370.67	2380.82
-60.00	57.71	2618.67	2628.82	-144.00	89.41	2534.67	2544.82	-226.00	112.01	2452.67	2462.82	-310.00	131.18	2368.67	2378.82
-62.00	58.67	2616.67	2626.82	-146.00	90.02	2532.67	2542.82	-228.00	112.50	2450.67	2460.82	-312.00	131.60	2366.67	2376.82
-64.00	59.60	2614.67	2624.82	-147.67	90.54	2531.00	2541.15	-230.00	112.99	2448.67	2458.82	-314.00	132.02	2364.67	2374.82

Hydraulic Investigations of the Erosion Potential of Flows Overtopping Owyhee Dam
8/25/2006

select y	PMF			select y	PMF			select y	PMF			select y	PMF		
	x lower	el. Lower	el. Upper		x lower	el. Lower	el. Upper		x lower	el. Lower	el. Upper		x lower	el. Lower	el. Upper
-66.00	60.53	2612.67	2622.82	-148.00	90.64	2530.67	2540.82	-232.00	113.48	2446.67	2456.82	-316.00	132.44	2362.67	2372.82
-68.00	61.44	2610.67	2620.82	-150.00	91.25	2528.67	2538.82	-234.00	113.97	2444.67	2454.82	-318.00	132.86	2360.67	2370.82
-70.00	62.34	2608.67	2618.82	-152.00	91.86	2526.67	2536.82	-236.00	114.46	2442.67	2452.82	-320.00	133.28	2358.67	2368.82
-72.00	63.22	2606.67	2616.82	-154.00	92.46	2524.67	2534.82	-238.00	114.94	2440.67	2450.82	-322.00	133.69	2356.67	2366.82
-74.00	64.09	2604.67	2614.82	-156.00	93.06	2522.67	2532.82	-240.00	115.42	2438.67	2448.82	-324.00	134.11	2354.67	2364.82
-76.00	64.95	2602.67	2612.82	-158.00	93.65	2520.67	2530.82	-242.00	115.90	2436.67	2446.82	-326.00	134.52	2352.67	2362.82
-78.00	65.80	2600.67	2610.82	-160.00	94.24	2518.67	2528.82	-244.00	116.38	2434.67	2444.82	-328.00	134.93	2350.67	2360.82
-80.00	66.64	2598.67	2608.82	-162.00	94.83	2516.67	2526.82	-246.00	116.86	2432.67	2442.82	-330.00	135.34	2348.67	2358.82
-82.00	67.47	2596.67	2606.82	-164.00	95.41	2514.67	2524.82	-248.00	117.33	2430.67	2440.82				

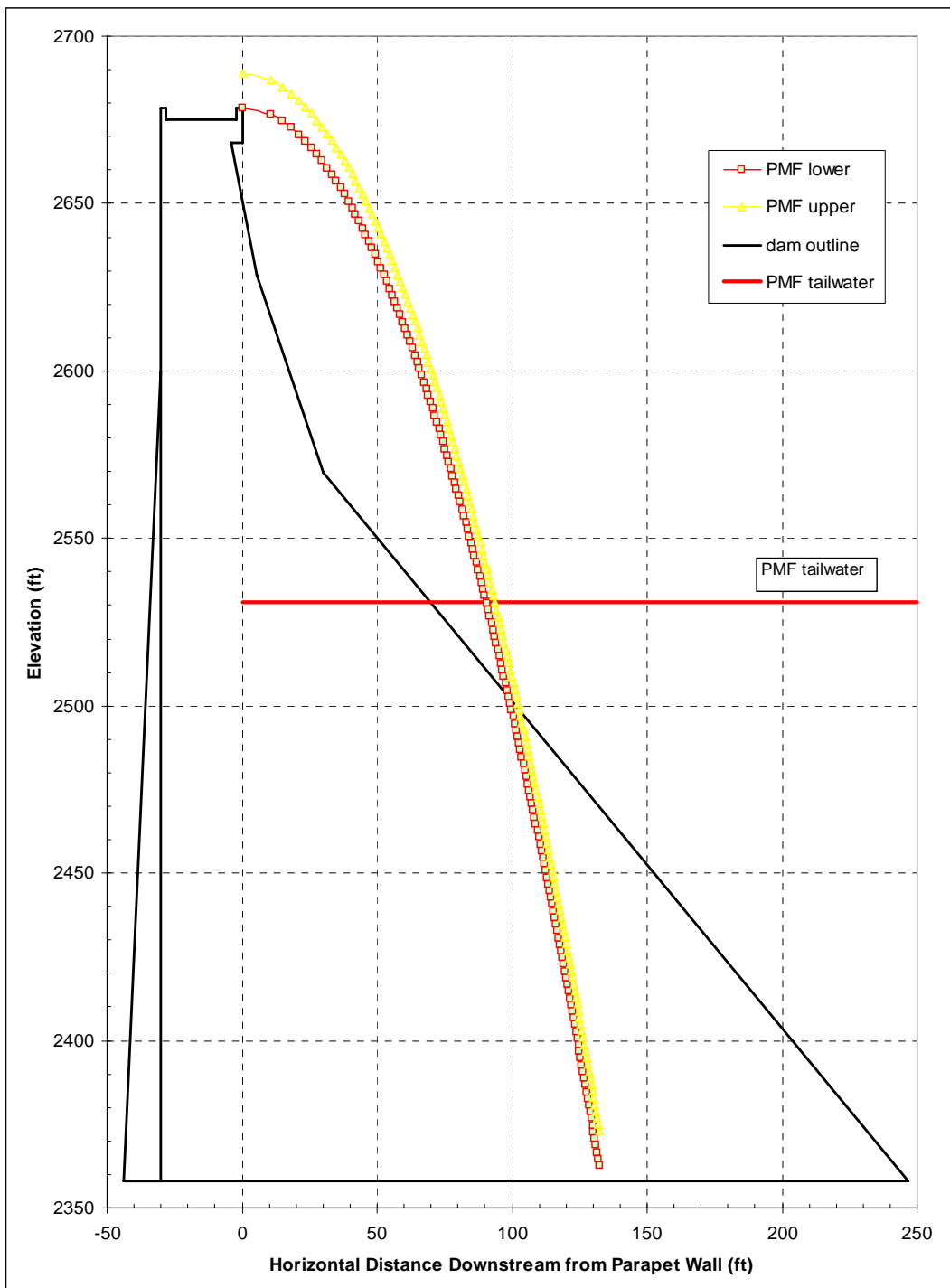


Figure 8. - Sectional view of the trajectory profile for the PMF flood event for Owyhee Dam through the maximum section aligned with the river channel.

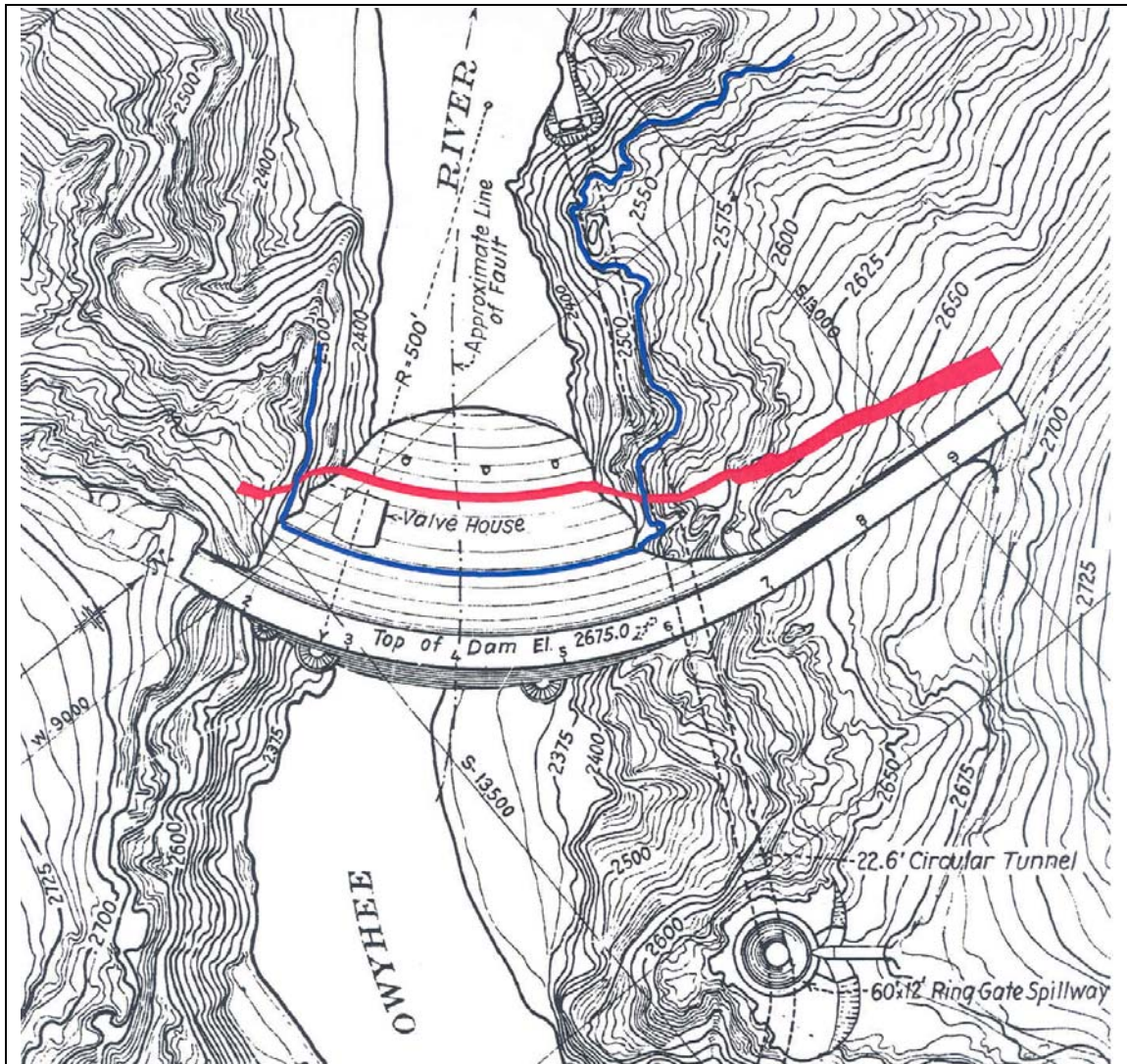


Figure 9. - Footprint of the trajectory with no spread of the jet for the PMF overtopping at Owyhee Dam. Note the location of the footprint does impact on the rock over the location of the spillway tunnel above the PMF tailwater shown in blue at El. 2531.

Jet Spread in the Free Fall and Potential for Jet Core Decay

The fall height of the jet varies across the width of the dam, depending on whether the jet impinges on the abutments or falls to the tailwater at El. 2531 for the PMF. The fall height is computed as the difference between the reservoir El. 2702.42 and the impingement location. In the case of fall to the tailwater the fall height, Z , is equal to 171.42 ft and is the maximum fall because the jet will impinge on the abutments sooner under the PMF.

There are three major flow regimes of a jet during a free fall. The flow regime at the brink of the fall over a dam is characterized by initial formation of waves on the surface, then the growth of

instabilities on the surface in the form of waves and vortices. The turbulence then grows as the surface vortices break down, aeration begins, and the jet begins spreading. The third regime is where the turbulent surface fluctuations are large enough to penetrate the core of the jet which leads to ultimate break up of the flow mass. During this process, the jet thickness is determined by the initial turbulence and the contraction of the jet due to gravitational acceleration. Jet break up refers to the spread of the outer edges of the jet as well as the potential for the surface turbulence to penetrate the core of the jet.

The initial turbulence of the jet will produce some spreading of the outer dimension of the jet, D_{out} , whether round or rectangular. If the free fall length, L_j , is enough, then aeration will begin prior to jet impingement on either the abutments or the tailwater pool. The length of fall of the jet break up, L_b , is also a function of the initial depth, velocity, turbulence intensity, and geometry of the release. The state of the development of the jet is dependent upon the comparison between the empirical equations determined to predict jet break up, L_b , and the length of the fall, L_j . In addition to aeration inception, the core of the jet may experience decay while free-falling if the turbulence is enough to penetrate the core of the jet. The jet will be broken up if the break up distance, L_b , is less than the fall distance, L_j , to the location of interest.

The following equations predict the dimension of the inner jet core and outer jet spread using empirical data from experiments based upon circular jets. For many applications, such as jets issuing from gates, the initial depth may be converted to an equivalent circular diameter and that parameter used for the initial depth, D_i . For overtopping, the footprint of the jet is expected to remain rectangular and the initial diameter of the jet is taken as the initial thickness of the rectangular jet, t_i . There is no extensive data for rectangular jets; therefore, the equations for round jets were applied for the analysis for Owyhee Dam with the rectangular jet thickness.

The contraction of the core of a round jet at the point of impingement or impact, D_j , due to gravity is computed for round jets by Bollaert [7] or using equation 5.46 from Annandale [8]:

$$D_j = D_i \sqrt{\frac{V_i}{V_j}}$$

where the D_i and V_i are the initial depth of overtopping and the initial velocity of the jet and V_j is the velocity at the location of impact. This equation is easily used to convert to a rectangular jet by using continuity to produce a jet thickness, t_j , at the point of impact given by:

$$t_j = t_i \left(\frac{V_i}{V_j} \right)$$

where the t_i and V_i are the initial brink depth and the initial velocity of the jet and V_j is the velocity at the location of impact. The velocity at the point of impact is given by equation 5.47 from Annandale [8] with Z equal to the total drop from the reservoir with gravitational effects:

$$V_j = \sqrt{V_i^2 + 2gZ}$$

Performing these two computations for Owyhee Dam at the impact with the tailwater produces a jet thickness, $t_j = 2.78$ ft and $V_j = 109.24$ ft/s. The spread of the outer portion of the jet, D_{out} , which includes aeration of a turbulent jet, has been computed by Ervine and Falvey [9] and Ervine et. al. [10] as equal to:

$$D_{out} = D_i + 2 * 0.38(T_u L_j)$$

where T_u is the turbulence intensity of the jet based upon values from table 4 for various types of jet issuance, and L_j is the length of the jet along the trajectory as it falls through the air to the impingement location. For an overtopping event, the jet diameter is replaced by the jet thickness and the characteristics of the thick jet overtopping the dam led to selection of a turbulence intensity, $T_u = 0.03$ from table 4. Inputting these values into the above equation for the dimension of the outer jet spread produces $D_{out} = 13.67$ ft at El. 2531 under the PMF event.

Table 4. - Table of turbulence intensities for free falling jets Bolleart (2002).

Structure type	Turbulence Intensity
free overfall	0.00-0.03
ski jump	0.03-0.05
Valve	0.03-0.08

For Owyhee Dam PMF overtopping the length of the trajectory to the tailwater, L_j , is 309 ft and is computed by equation 5.37 from Annandale [8] integrated to horizontal distance x :

$$L_j = x \sqrt{1 + \left[\tan \theta - \frac{2x}{4Kh_v \cos^2 \theta} \right]^2}$$

where K is a constant used to account for jet turbulence and is equal to 1, a conservative assumption regarding jet turbulence. The trajectory length may also just be computed geometrically. The jet characteristics for the free-fall (and the later plunge into the tailwater pool) are given in table 5.

The following equations, from Ervine, et al. [10], were used to determine the length to the expected break up of the jet as it falls through the air, L_b :

$$C^2 = \frac{1}{\left(\frac{2L_b}{t_i F_{ri}^2} + 1 \right) * \left(\sqrt{\frac{2L_b}{t_i F_{ri}^2} + 1} - 1 \right)^2}$$

$$\text{where } C = 1.14 T_u F_{ri}^2$$

where F_{ri} is equal to the Froude number at the brink depth. Again, the turbulence intensity is selected from table 4 as 0.03. The result of this computation is that the length of free fall for break up of the jet core, L_b , is equal to 185 ft for the PMF event.

Jet break up implies that the flow no longer is a coherent mass of water and thus will add little or no additional impact pressure to the surface upon impingement. Therefore, the stream power will only be a function of the force imparted by the falling mass of water spread as computed, but no additional pressure fluctuations need be considered.

Another method has been proposed for predicting jet break up of the core of a rectangular jet defined as:

$$L_b = 6 * q^{0.32}$$

The break up length for the PMF at Owyhee Dam would be 37 ft. This does not seem practical as the initial jet thickness at the brink is 10.15 ft.

The other end of the spectrum for predicting the length to decay of the jet core and break up is given by:

$$L_b = 50 - 100D_i$$

developed from circular jet experiments by Falvey and Ervine [9]. For the Owyhee Dam PMF event, the predicted fall till jet break up would be 500 to 1000 ft, thus the core would be intact for the available fall below Owyhee Dam.

Comparison of these methods points out that there is quite a bit of potential uncertainty in the result and judgement is required to apply equations for round jets to an overtopping situation. The trajectory length of fall to the PMF tailwater is 309 ft, therefore; using the equation that includes the turbulence intensity and initial velocity predicts that the jet will break up prior to plunging into the tailwater and the jet is fully developed. Converting the fall length along the trajectory of 185 ft to a vertical elevation, the jet will be broken up by the time it impinges on the rock abutments at El. 2593.

Jet Trajectories for Various Overtopping Flows

Investigation of the jet trajectories for other flood events was performed for use, if needed; in risk determination of other than erosion under the PMF is requested. The discharges and initial reservoir elevations for flood frequencies of 5000, 10000, 20000, 50000, 1000000 -year events, shown in table 1 of this report, from the Flood Routing TM were used [3].

The horizontal (x) and vertical (y) distances are given from the downstream dam parapet wall. The lower nappe begins at the elevation of the parapet wall, El. 2678.67 and is computed using the horizontal and vertical displacements from the equation of projectile motion. The upper nappe was determined by adding the initial overtopping brink depth to the lower nappe elevation. Figure 10 shows the family of trajectories determined for the various flood frequencies, including the previous result for the PMF. The supporting trajectory data are given in the appendix and were used to determine stream power and erodibility potential for other flood events.

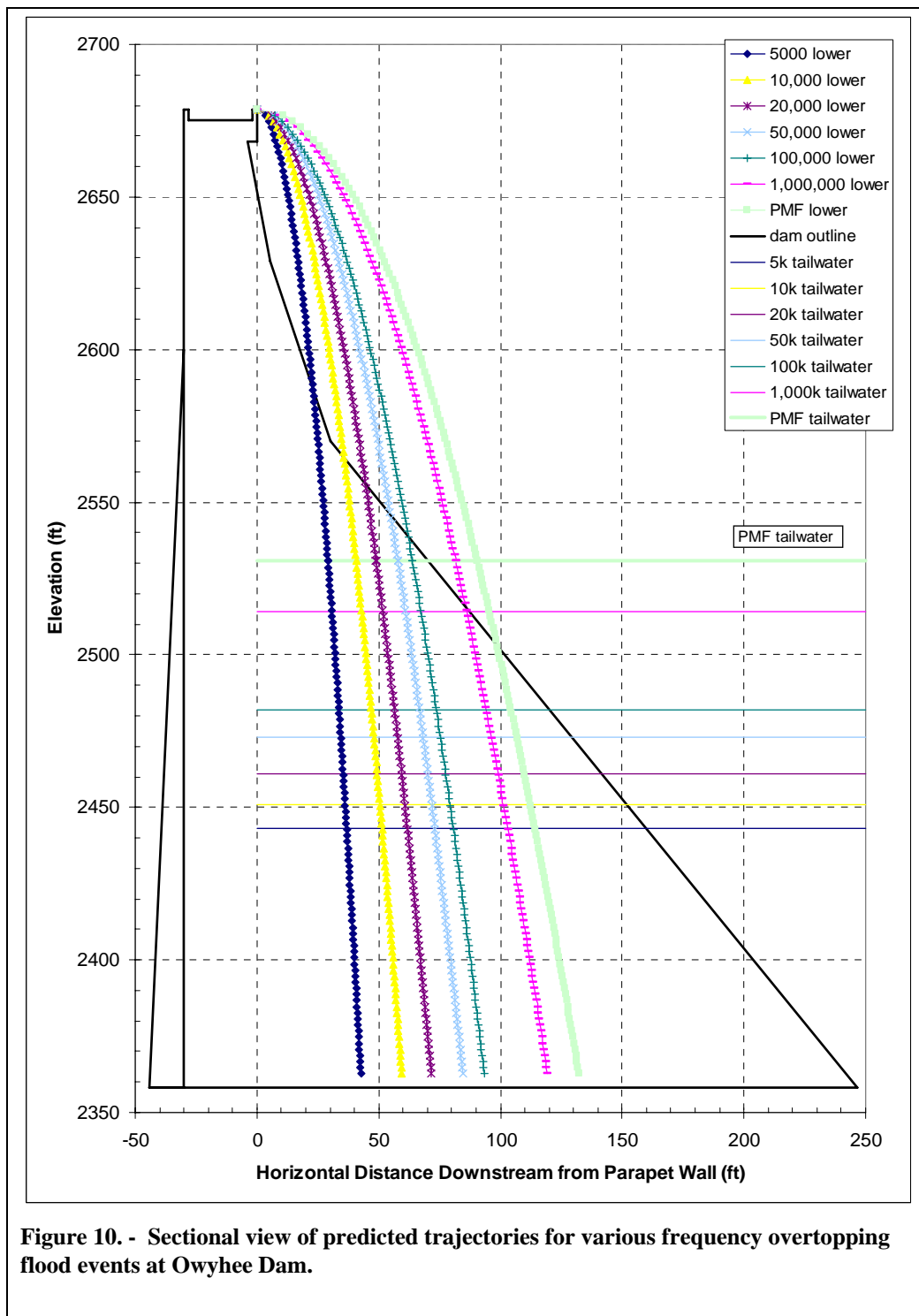
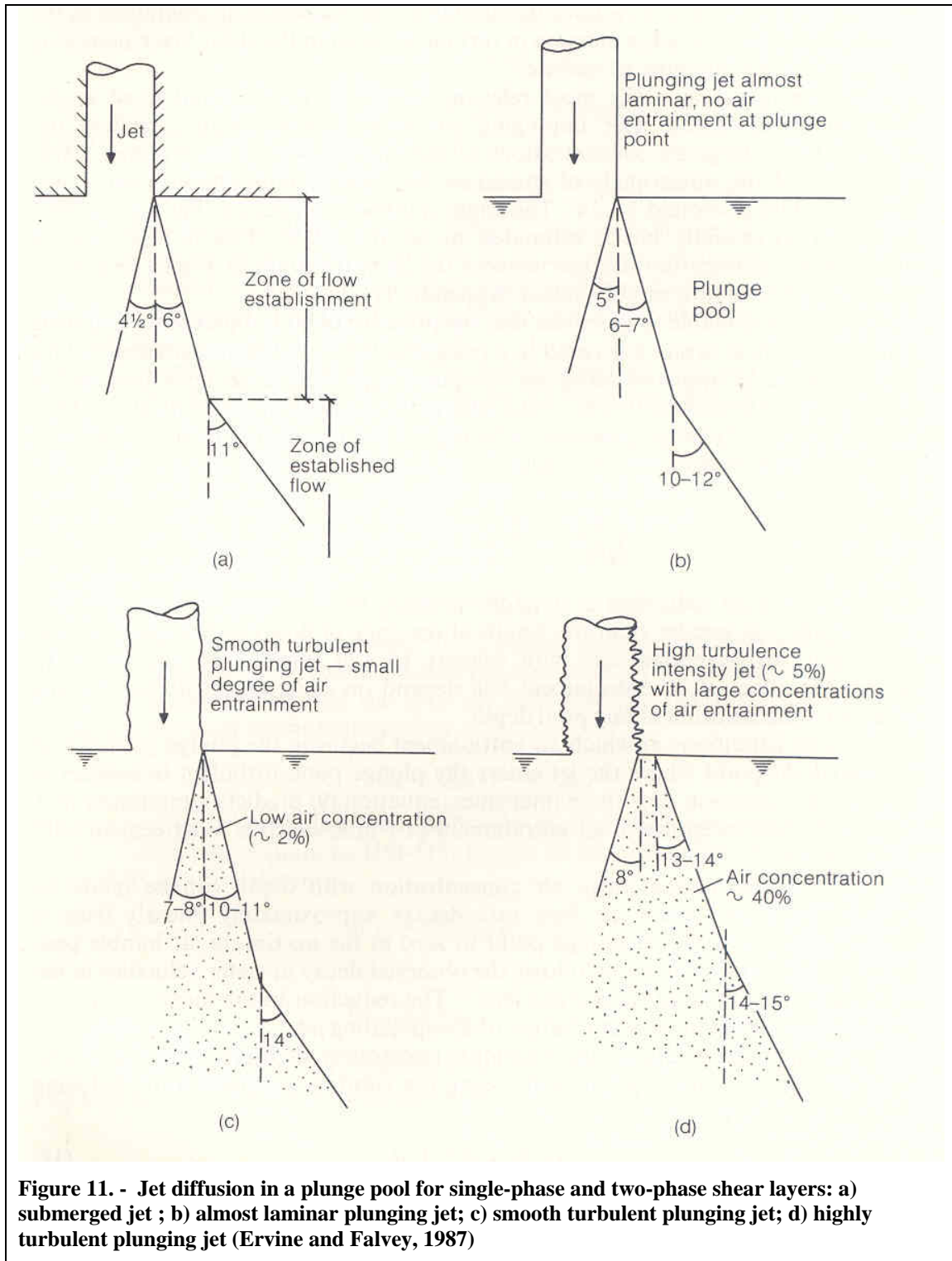


Figure 10. - Sectional view of predicted trajectories for various frequency overtopping flood events at Owyhee Dam.

Jet Plunge Pool Characteristics

The next portion of the investigation is to determine the characteristics of the jet as it travels into and through the plunge pool as shown on figure 11.



The previous section described the jet characteristics through the free fall. Depending upon which equation is used to determine break up of the jet core, the core may or may not be intact when the jet plunges into the tailwater pool. Even though it is felt that the jet will be fully developed and no core will still exist for the Owyhee Dam PMF, this analysis was performed with a core jet assumed. The data for the free falling jet show the impingement angle to be greater than 70 degrees at the tailwater. Investigations [7, 8] have shown that for impingement angles greater than 70 degrees not adjustment need be made for the path of the jet through the pool.

Figure 11 shows how the core of a jet will diffuse or decay or contract until the energy no longer remains to impact a surface and the outside of the jet will disperse if there is adequate depth. Both the core and outer diameter of the jet will change as a function of the initial velocity and turbulence. The selection of the jet characteristics prior to impingement with the tailwater surface will produce a consequence on the expected extent of the jet. A sensitivity analysis was not performed for this application. It was assumed that the core would diffuse at an angle of 8 degrees as it plunges through the tailwater. Performing the calculation determined that the core of the jet would be fully diffused in about 10 ft. Therefore, there will be no further impact from the core of the jet on the rock of the abutments in the tailwater pool below about El. 2521.

The outer edges of the jet will spread at an angle of 6 to 14 degrees depending upon the initial turbulence level of the jet. The outer edge of the jet for Owyhee Dam was assumed to spread at an angle of 14 degrees. As the jet spreads, the extent of the impact zone on the rock abutment will increase. Table 5 shows the jet characteristics for the PMF overtopping at Owyhee Dam both above and below the tailwater after a vertical fall distance below the dam parapet wall of 316 ft, or just about the predicted foundation elevation at the toe of the dam.

Table 5. - Jet characteristics for the PMF overtopping of Owyhee Dam including both the free-falling jet and the jet below the tailwater.

Vertical distance (y) from parapet elevation (ft)	Horizontal distance (x) from downstream parapet	Elevation of lower nappe (ft)	Elevation of upper nappe (ft)	Trajectory length (ft)	Velocity of jet at impact with various elevations. (ft/s)	Jet angle of impingement (degrees)	Outer width of jet above and below tailwater (ft)	Rectangular jet core dimensions above and below the tailwater (ft)
0.00	0.00	2678.67	2688.82	0.00	49.23	10.75	10.15	6.16
-2.00	10.54	2676.67	2686.82	11.27	50.52	24.62	10.27	6.00
-4.00	14.90	2674.67	2684.82	16.91	51.78	30.85	10.34	5.86
-6.00	18.25	2672.67	2682.82	21.84	53.01	35.31	10.39	5.72
-8.00	21.07	2670.67	2680.82	26.46	54.21	38.80	10.45	5.59
-10.00	23.56	2668.67	2678.82	30.90	55.38	41.65	10.50	5.48
-12.00	25.81	2666.67	2676.82	35.24	56.53	44.04	10.55	5.36
-14.00	27.88	2664.67	2674.82	39.51	57.66	46.10	10.60	5.26
-16.00	29.80	2662.67	2672.82	43.73	58.77	47.89	10.64	5.16
-18.00	31.61	2660.67	2670.82	47.91	59.85	49.47	10.69	5.07
-20.00	33.32	2658.67	2668.82	52.06	60.92	50.88	10.74	4.98
-22.00	34.95	2656.67	2666.82	56.19	61.97	52.15	10.79	4.89
-24.00	36.50	2654.67	2664.82	60.30	63.00	53.31	10.83	4.81
-26.00	37.99	2652.67	2662.82	64.40	64.01	54.36	10.88	4.74
-28.00	39.42	2650.67	2660.82	68.49	65.01	55.32	10.93	4.67
-30.00	40.81	2648.67	2658.82	72.56	65.99	56.21	10.97	4.60
-32.00	42.15	2646.67	2656.82	76.63	66.96	57.03	11.02	4.53
-34.00	43.44	2644.67	2654.82	80.69	67.92	57.80	11.06	4.47
-36.00	44.70	2642.67	2652.82	84.75	68.86	58.51	11.11	4.40
-38.00	45.93	2640.67	2650.82	88.80	69.79	59.18	11.16	4.35
-40.00	47.12	2638.67	2648.82	92.85	70.71	59.81	11.20	4.29
-42.00	48.28	2636.67	2646.82	96.89	71.61	60.40	11.25	4.24
-44.00	49.42	2634.67	2644.82	100.93	72.50	60.95	11.30	4.18
-46.00	50.53	2632.67	2642.82	104.96	73.39	61.48	11.34	4.13
-48.00	51.62	2630.67	2640.82	109.00	74.26	61.98	11.39	4.08
-50.00	52.68	2628.67	2638.82	113.03	75.12	62.45	11.43	4.04
-52.00	53.73	2626.67	2636.82	117.06	75.97	62.90	11.48	3.99
-54.00	54.75	2624.67	2634.82	121.08	76.82	63.33	11.53	3.95
-56.00	55.75	2622.67	2632.82	125.11	77.65	63.74	11.57	3.91

Vertical distance (y) from parapet elevation (ft)	Horizontal distance (x) from downstream parapet	Elevation of lower nappe (ft)	Elevation of upper nappe (ft)	Trajectory length (ft)	Velocity of jet at impact with various elevations. (ft/s)	Jet angle of impingement (degrees)	Outer width of jet above and below tailwater (ft)	Rectangular jet core dimensions above and below the tailwater (ft)
-58.00	56.74	2620.67	2630.82	129.13	78.48	64.13	11.62	3.86
-60.00	57.71	2618.67	2628.82	133.16	79.29	64.50	11.66	3.82
-62.00	58.67	2616.67	2626.82	137.18	80.10	64.86	11.71	3.79
-64.00	59.60	2614.67	2624.82	141.20	80.90	65.20	11.75	3.75
-66.00	60.53	2612.67	2622.82	145.22	81.69	65.53	11.80	3.71
-68.00	61.44	2610.67	2620.82	149.23	82.48	65.84	11.85	3.68
-70.00	62.34	2608.67	2618.82	153.25	83.25	66.15	11.89	3.64
-72.00	63.22	2606.67	2616.82	157.27	84.02	66.44	11.94	3.61
-74.00	64.09	2604.67	2614.82	161.28	84.79	66.72	11.98	3.58
-76.00	64.95	2602.67	2612.82	165.30	85.54	67.00	12.03	3.55
-78.00	65.80	2600.67	2610.82	169.31	86.29	67.26	12.08	3.51
-80.00	66.64	2598.67	2608.82	173.32	87.04	67.51	12.12	3.48
-82.00	67.47	2596.67	2606.82	177.34	87.77	67.76	12.17	3.46
-84.00	68.28	2594.67	2604.82	181.35	88.50	68.00	12.21	3.43
-86.00	69.09	2592.67	2602.82	185.36	89.23	68.23	12.26	3.40
-88.00	69.89	2590.67	2600.82	189.37	89.95	68.45	12.30	3.37
-90.00	70.68	2588.67	2598.82	193.38	90.66	68.67	12.35	3.35
-92.00	71.46	2586.67	2596.82	197.39	91.37	68.88	12.40	3.32
-94.00	72.24	2584.67	2594.82	201.40	92.07	69.08	12.44	3.29
-96.00	73.00	2582.67	2592.82	205.41	92.77	69.28	12.49	3.27
-98.00	73.76	2580.67	2590.82	209.42	93.46	69.47	12.53	3.25
-100.00	74.50	2578.67	2588.82	213.43	94.14	69.66	12.58	3.22
-102.00	75.25	2576.67	2586.82	217.43	94.83	69.84	12.62	3.20
-104.00	75.98	2574.67	2584.82	221.44	95.50	70.02	12.67	3.18
-106.00	76.71	2572.67	2582.82	225.45	96.17	70.19	12.72	3.15
-108.00	77.43	2570.67	2580.82	229.46	96.84	70.36	12.76	3.13
-110.00	78.14	2568.67	2578.82	233.47	97.50	70.53	12.81	3.11
-112.00	78.85	2566.67	2576.82	237.47	98.16	70.69	12.85	3.09
-114.00	79.55	2564.67	2574.82	241.48	98.82	70.84	12.90	3.07
-116.00	80.24	2562.67	2572.82	245.49	99.47	71.00	12.94	3.05
-118.00	80.93	2560.67	2570.82	249.49	100.11	71.15	12.99	3.03

Hydraulic Investigations of the Erosion Potential of Flows Overtopping Owyhee Dam
8/25/2006

Vertical distance (y) from parapet elevation (ft)	Horizontal distance (x) from downstream parapet	Elevation of lower nappe (ft)	Elevation of upper nappe (ft)	Trajectory length (ft)	Velocity of jet at impact with various elevations. (ft/s)	Jet angle of impingement (degrees)	Outer width of jet above and below tailwater (ft)	Rectangular jet core dimensions above and below the tailwater (ft)
-120.00	81.62	2558.67	2568.82	253.50	100.75	71.29	13.03	3.01
-122.00	82.29	2556.67	2566.82	257.50	101.39	71.43	13.08	2.99
-124.00	82.96	2554.67	2564.82	261.51	102.02	71.57	13.13	2.97
-126.00	83.63	2552.67	2562.82	265.51	102.65	71.71	13.17	2.95
-128.00	84.29	2550.67	2560.82	269.52	103.28	71.84	13.22	2.94
-130.00	84.95	2548.67	2558.82	273.53	103.90	71.97	13.26	2.92
-132.00	85.60	2546.67	2556.82	277.53	104.52	72.10	13.31	2.90
-134.00	86.25	2544.67	2554.82	281.54	105.13	72.22	13.35	2.88
-136.00	86.89	2542.67	2552.82	285.54	105.74	72.35	13.40	2.87
-138.00	87.52	2540.67	2550.82	289.55	106.35	72.46	13.45	2.85
-140.00	88.16	2538.67	2548.82	293.55	106.95	72.58	13.49	2.84
-142.00	88.78	2536.67	2546.82	297.55	107.55	72.70	13.54	2.82
-144.00	89.41	2534.67	2544.82	301.56	108.15	72.81	13.58	2.80
-146.00	90.02	2532.67	2542.82	305.56	108.75	72.91	13.63	2.79
-147.67	90.54	2531.00	2541.15	308.91	109.24	72.97	13.67	2.78
-148.00	90.64	2530.67	2540.82	309.57	109.34	73.03	13.78	2.68
-150.00	91.25	2528.67	2538.82	313.57	109.92	73.13	14.49	2.12
-152.00	91.86	2526.67	2536.82	317.57	110.51	73.24	15.19	1.56
-154.00	92.46	2524.67	2534.82	321.58	111.09	73.34	15.90	1.00
-156.00	93.06	2522.67	2532.82	325.58	111.67	73.44	16.60	0.43
-158.00	93.65	2520.67	2530.82	329.59	112.24	73.54	17.31	-0.13
-160.00	94.24	2518.67	2528.82	333.59	112.81	73.64	18.01	0.00
-162.00	94.83	2516.67	2526.82	337.59	113.38	73.73	18.72	0.00
-164.00	95.41	2514.67	2524.82	341.60	113.95	73.83	19.43	0.00
-166.00	95.99	2512.67	2522.82	345.60	114.51	73.92	20.13	0.00
-168.00	96.57	2510.67	2520.82	349.60	115.08	74.01	20.84	0.00
-170.00	97.14	2508.67	2518.82	353.61	115.63	74.10	21.54	0.00
-172.00	97.71	2506.67	2516.82	357.61	116.19	74.19	22.25	0.00
-174.00	98.28	2504.67	2514.82	361.61	116.74	74.27	22.95	0.00
-176.00	98.84	2502.67	2512.82	365.61	117.29	74.36	23.66	0.00
-178.00	99.40	2500.67	2510.82	369.62	117.84	74.44	24.36	0.00

Vertical distance (y) from parapet elevation (ft)	Horizontal distance (x) from downstream parapet	Elevation of lower nappe (ft)	Elevation of upper nappe (ft)	Trajectory length (ft)	Velocity of jet at impact with various elevations. (ft/s)	Jet angle of impingement (degrees)	Outer width of jet above and below tailwater (ft)	Rectangular jet core dimensions above and below the tailwater (ft)
-180.00	99.96	2498.67	2508.82	373.62	118.39	74.52	25.07	0.00
-182.00	100.51	2496.67	2506.82	377.62	118.93	74.60	25.77	0.00
-184.00	101.06	2494.67	2504.82	381.63	119.47	74.68	26.48	0.00
-186.00	101.61	2492.67	2502.82	385.63	120.01	74.76	27.18	0.00
-188.00	102.16	2490.67	2500.82	389.63	120.54	74.84	27.89	0.00
-190.00	102.70	2488.67	2498.82	393.63	121.08	74.91	28.59	0.00
-192.00	103.24	2486.67	2496.82	397.64	121.61	74.99	29.30	0.00
-194.00	103.77	2484.67	2494.82	401.64	122.13	75.06	30.01	0.00
-196.00	104.31	2482.67	2492.82	405.64	122.66	75.14	30.71	0.00
-198.00	104.84	2480.67	2490.82	409.64	123.18	75.21	31.42	0.00
-200.00	105.37	2478.67	2488.82	413.64	123.71	75.28	32.12	0.00
-202.00	105.89	2476.67	2486.82	417.65	124.23	75.35	32.83	0.00
-204.00	106.41	2474.67	2484.82	421.65	124.74	75.42	33.53	0.00
-206.00	106.93	2472.67	2482.82	425.65	125.26	75.48	34.24	0.00
-208.00	107.45	2470.67	2480.82	429.65	125.77	75.55	34.94	0.00
-210.00	107.97	2468.67	2478.82	433.66	126.28	75.62	35.65	0.00
-212.00	108.48	2466.67	2476.82	437.66	126.79	75.68	36.35	0.00
-214.00	108.99	2464.67	2474.82	441.66	127.30	75.75	37.06	0.00
-216.00	109.50	2462.67	2472.82	445.66	127.80	75.81	37.76	0.00
-218.00	110.00	2460.67	2470.82	449.66	128.31	75.87	38.47	0.00
-220.00	110.51	2458.67	2468.82	453.67	128.81	75.93	39.17	0.00
-222.00	111.01	2456.67	2466.82	457.67	129.31	75.99	39.88	0.00
-224.00	111.51	2454.67	2464.82	461.67	129.80	76.05	40.58	0.00
-226.00	112.01	2452.67	2462.82	465.67	130.30	76.11	41.29	0.00
-228.00	112.50	2450.67	2460.82	469.67	130.79	76.17	42.00	0.00
-230.00	112.99	2448.67	2458.82	473.67	131.28	76.23	42.70	0.00
-232.00	113.48	2446.67	2456.82	477.68	131.77	76.29	43.41	0.00
-234.00	113.97	2444.67	2454.82	481.68	132.26	76.34	44.11	0.00
-236.00	114.46	2442.67	2452.82	485.68	132.75	76.40	44.82	0.00
-238.00	114.94	2440.67	2450.82	489.68	133.23	76.45	45.52	0.00
-240.00	115.42	2438.67	2448.82	493.68	133.71	76.51	46.23	0.00

Hydraulic Investigations of the Erosion Potential of Flows Overtopping Owyhee Dam
8/25/2006

Vertical distance (y) from parapet elevation (ft)	Horizontal distance (x) from downstream parapet	Elevation of lower nappe (ft)	Elevation of upper nappe (ft)	Trajectory length (ft)	Velocity of jet at impact with various elevations. (ft/s)	Jet angle of impingement (degrees)	Outer width of jet above and below tailwater (ft)	Rectangular jet core dimensions above and below the tailwater (ft)
-242.00	115.90	2436.67	2446.82	497.68	134.19	76.56	46.93	0.00
-244.00	116.38	2434.67	2444.82	501.69	134.67	76.61	47.64	0.00
-246.00	116.86	2432.67	2442.82	505.69	135.15	76.67	48.34	0.00
-248.00	117.33	2430.67	2440.82	509.69	135.63	76.72	49.05	0.00
-250.00	117.80	2428.67	2438.82	513.69	136.10	76.77	49.75	0.00
-252.00	118.27	2426.67	2436.82	517.69	136.57	76.82	50.46	0.00
-254.00	118.74	2424.67	2434.82	521.69	137.04	76.87	51.16	0.00
-256.00	119.21	2422.67	2432.82	525.69	137.51	76.92	51.87	0.00
-258.00	119.67	2420.67	2430.82	529.70	137.98	76.97	52.57	0.00
-260.00	120.14	2418.67	2428.82	533.70	138.45	77.02	53.28	0.00
-262.00	120.60	2416.67	2426.82	537.70	138.91	77.06	53.99	0.00
-264.00	121.06	2414.67	2424.82	541.70	139.37	77.11	54.69	0.00
-266.00	121.51	2412.67	2422.82	545.70	139.83	77.16	55.40	0.00
-268.00	121.97	2410.67	2420.82	549.70	140.29	77.20	56.10	0.00
-270.00	122.42	2408.67	2418.82	553.70	140.75	77.25	56.81	0.00
-272.00	122.88	2406.67	2416.82	557.70	141.21	77.29	57.51	0.00
-274.00	123.33	2404.67	2414.82	561.71	141.66	77.34	58.22	0.00
-276.00	123.78	2402.67	2412.82	565.71	142.12	77.38	58.92	0.00
-278.00	124.22	2400.67	2410.82	569.71	142.57	77.43	59.63	0.00
-280.00	124.67	2398.67	2408.82	573.71	143.02	77.47	60.33	0.00
-282.00	125.11	2396.67	2406.82	577.71	143.47	77.51	61.04	0.00
-284.00	125.56	2394.67	2404.82	581.71	143.92	77.56	61.74	0.00
-286.00	126.00	2392.67	2402.82	585.71	144.37	77.60	62.45	0.00
-288.00	126.44	2390.67	2400.82	589.71	144.81	77.64	63.15	0.00
-290.00	126.88	2388.67	2398.82	593.72	145.26	77.68	63.86	0.00
-292.00	127.31	2386.67	2396.82	597.72	145.70	77.72	64.57	0.00
-294.00	127.75	2384.67	2394.82	601.72	146.14	77.76	65.27	0.00
-296.00	128.18	2382.67	2392.82	605.72	146.58	77.80	65.98	0.00
-298.00	128.62	2380.67	2390.82	609.72	147.02	77.84	66.68	0.00
-300.00	129.05	2378.67	2388.82	613.72	147.46	77.88	67.39	0.00
-302.00	129.48	2376.67	2386.82	617.72	147.89	77.92	68.09	0.00

Vertical distance (y) from parapet elevation (ft)	Horizontal distance (x) from downstream parapet	Elevation of lower nappe (ft)	Elevation of upper nappe (ft)	Trajectory length (ft)	Velocity of jet at impact with various elevations. (ft/s)	Jet angle of impingement (degrees)	Outer width of jet above and below tailwater (ft)	Rectangular jet core dimensions above and below the tailwater (ft)
-304.00	129.90	2374.67	2384.82	621.72	148.33	77.96	68.80	0.00
-306.00	130.33	2372.67	2382.82	625.72	148.76	78.00	69.50	0.00
-308.00	130.76	2370.67	2380.82	629.72	149.19	78.03	70.21	0.00
-310.00	131.18	2368.67	2378.82	633.73	149.62	78.07	70.91	0.00
-312.00	131.60	2366.67	2376.82	637.73	150.05	78.11	71.62	0.00
-314.00	132.02	2364.67	2374.82	641.73	150.48	78.15	72.32	0.00
-316.00	132.44	2362.67	2372.82	645.73	150.91	67.26	73.03	0.00

Shaded row indicates the location of the tailwater elevation at the PMF.

Rock Erodibility and Stream Power

Figure 9 shows the predicted footprint of the jet at it would impinge on the rock abutments and into the tailwater. The question of whether the rock will erode is discussed in the following sections based upon the method proposed by Annandale [8].

Rock Erodibility

The erodibility index is a geomechanical index that is used to quantify the relative ability of earth and engineered earth materials to resist the erosive capacity of water [8]. The erodibility indices for the rock abutments at Owyhee Dam and the following discussion were provided by Joseph Kottenstette, Geotechnical Engineer, 86-68110, US Bureau of Reclamation, Technical Services Center.

Five factors are considered in the erodibility index:

M_s : Material strength or Mass strength	Range 0.45-250
K_b : Block Size RQD/J_n	Range J_n 1-5; RQD 0-100 i.e. 0-100
K_d : Shear strength of joints J_r/J_a	Range J_r 1-4; J_a 0.75-18 i.e. 0.2-18
J_s : Relative ground structure number	Range 0.37-1.00

The overall erodibility index, K , is the product of these four factors. All of these factors are important; however, this method may not distribute the appropriate proportion of each component to the overall factor in a way that is consistent with rock mechanics and the stability in rock masses. Based on the ranges of values for these factors it is easy to see that the two dominant factors, M_s and K_b , are arguably over valued. In most stability problems involving rock masses it is the joint orientations relative to the free face, the direction of the load, and the shear strength of the joints, that are often dominant parameters. The factors K_d and J_s address these features better in rock masses and therefore, should carry the most weight for the hard rock condition at Owyhee and at most Reclamation concrete dam sites. In addition, these rock features are not handled in a 3-D framework, nor does the method developed by Annandale [8] address the concept of resolvability. These can potentially be serious shortcomings. Also, the empirical line defining the boundary between erosion and no erosion, as a function of the stream power and erodibility index, is dominated by data from low energy stream power conditions on weak soil-lined channels. This line might, therefore, apply best to conditions that are dominated by the mass strength factor, M_s . In most cases for plunge pools and concrete dam abutments, the mass strength factor could be considered constant because most are founded in hard rock formations at the high end of the strength range.

This does not mean that we cannot evaluate the erosion potential at Owyhee Dam. It does mean that we need to look closely at all the information that is available and make a judgment call for the abutments at Owyhee. The following descriptions may be as convincing as the erodibility index and should be considered very carefully when performing a sensitivity analysis or using the erodibility index versus stream power graph when determining probability of erosion and potential failure in a risk assessment venue.

The river has eroded a very deep canyon into the rhyolite foundation. The canyon walls are very steep and might lead one to think that they would be resistant to erosion; however, this thought is erroneous. The canyon and river channel follow a very continuous relatively wide (10s of feet) fracture zone in the rhyolite foundation material. This zone is clearly more erodible than the rest of the rhyolite. The fracture system in the rhyolite is dominated by flow banding and a related fracture system that is primarily vertical and horizontal or near horizontal. The fractures are rough and clean giving them a relatively high strength.

The fracture system creates many relatively small removable blocks. As the river eroded the weaker central fracture zone it continued to erode rock on either side of the canyon until the reduced velocities of the wider channel could no longer erode the canyon walls. This process continued over a long time to produce the canyon we see today. The dominant load currently on the canyon walls is gravity resulting in a system of relatively small blocks that are quite stable under gravity loads producing the steep canyon.

We have since built the dam storing both massive amounts of water and potential energy behind the dam. In an overtopping event, the extreme change in hydraulic gradient will release this energy onto the rock abutments and the loads change from gravity to some very high hydraulic pressures that will de-stabilize the rhyolite blocks in the canyon walls at the location of the impinging jet produced by the overtopping flows.

The primary factor that controlled the erodibility index number was the RQD number based on two drill holes. This number is related to block size and in the upper abutments of Owyhee Dam the RQD values were very low. The rock strength numbers also play a large roll in the erodibility index and the upper right abutment has 20 feet of weak Tuff rock unit in the drill hole. This rock type could be confined to a relatively small area or it may be more extensive. It is difficult to tell because the surface geology map shows large areas that are covered by overburden and prevents accurate mapping of the contact between the tuff and the rhyolite.

The physical evidence described above indicates the abutments of Owyhee dam might be very erodible. The erodibility index can be misleading, as was pointed out in the first part of this description, and in this case it may over estimate the index except for the fact that the RQD was zero in many locations. Nevertheless the overall erodibility index, K, was estimated and is shown in table 6 for various rock depths at Owyhee Dam.

Table 6. - Estimated erodibility indices and critical stream power values for the surface downstream from Owyhee Dam (per Kottenstette, 2006, personnel communication).

Material	Erodibility Index (K)	Threshold Stream Power Density (kW/m ²) (P _c)
right abutment surface (0-20 ft)	112.5	34.54
right abutment surface (0- 20 ft)	450	97.70
right abutment upper (57-89 ft)	1746	270.11
right abutment lower (89-150 ft)	4356	536.19
left abutment surface (1.5-38 ft)	21018	1745.60

Material	Erodibility Index (K)	Threshold Stream Power Density (kW/m ²) (P _c)
left abutment lower (38-150 ft)	11048	1077.61

The extent of erosion for overtopping flows is determined based upon comparison of the erodibility and the available energy according to Annandale's method [8].

Erosion Potential

Now that the jet characteristics and rock erodibility have been estimated, the potential for erosion may be determined. The erosion potential may be quantified by determining the erosive stream power. The stream power is the rate at which energy is applied after the jet has travelled through a vertical distance, Z, to a location on a surface or in a pool:

$$P_{jet} = \gamma QZ$$

where P_{jet} is the total stream power of the jet, γ is the unit weight of water, and Q is the total discharge. The stream power per unit area is determined by dividing the total stream power by the footprint of the area of the jet at the point of impact. This stream power per unit area or stream power density of the jet is:

$$p_{jet} = \frac{\gamma QZ}{A_i}$$

and may be used to determine whether erosion will occur or not as a function of the erodibility of the material or rock. The unit area of the jet changes with the fall both above and below the tailwater and is based upon the characteristics of the jet, including the spread and angle of jet impingement. There is a limit or threshold of erosion based upon a body of empirical data.

A threshold of erodibility has been defined as a function of the erodibility index, K as follows [8]:

$$P_c = K^{0.75} \quad \text{for higher erodibility or } K > 0.1$$

$$P_c = 0.48K^{0.44} \quad \text{for less erodibility or } K < 0.1$$

The threshold stream power densities were computed for the K values for Owyhee Dam and are also shown in table 6. Erosion will occur for conditions exceeding the "erosion threshold line" computed with the equation for K > 0.1 for Owyhee Dam. It was assumed that the rock material given for the lower elevations of the right and left abutments will continue down to the base of the foundation at the dam toe.

The stream power was computed for the PMF event that produced an overtopping brink depth and unit discharge of 10.15 ft and 303 ft³/s/ft with the jet characteristics as determined in the previous sections and shown in table 5. The stream power was computed both above and below the PMF tailwater at El. 2531. The jet characteristics determine the outer footprint of the jet as it would impact on the rock abutments enter into the tailwater pool. As a worst case assumption that the core of the jet will remain at the pool, it would then dissipate through the pool and no longer produce additional impact after elevation 2521, but the extent of the jet will still produce impact below the tailwater. At impact with the tailwater pool, the outer dimension of the jet has spread to 13.67 ft and will continue spreading through the pool, thus decreasing the stream power per unit area, as expected. The results of the stream power per unit area computations are shown in table 7 with the stream power from the last column plotted on figure 12.

Table 7. - Stream power in the flow and the width of the jet per unit area at various elevations below Owyhee Dam. The area of the jet is determined from the outer jet thickness of a unit width of flow.

El. of Jet underside (ft)	Area of jet footprint (ft ²)	Stream power density (ft-lb/s/ft)	Stream power density (ft-lb/s-ft ²)	Stream power density (HP/ft ²)	Stream power density (kW/m ²)
2678.67	10.15	449820	44339	81	647
2676.67	10.27	487699	47471	86	693
2674.67	10.34	525579	50840	92	742
2672.67	10.39	563459	54210	99	791
2670.67	10.45	601338	57562	105	840
2668.67	10.50	639218	60893	111	889
2666.67	10.55	677097	64199	117	937
2664.67	10.60	714977	67479	123	985
2662.67	10.64	752856	70733	129	1032
2660.67	10.69	790736	73961	134	1079
2658.67	10.74	828616	77163	140	1126
2656.67	10.79	866495	80338	146	1172
2654.67	10.83	904375	83487	152	1218
2652.67	10.88	942254	86610	157	1264
2650.67	10.93	980134	89708	163	1309
2648.67	10.97	1018013	92780	169	1354
2646.67	11.02	1055893	95827	174	1398
2644.67	11.06	1093772	98850	180	1443
2642.67	11.11	1131652	101848	185	1486
2640.67	11.16	1169532	104821	191	1530
2638.67	11.20	1207411	107771	196	1573
2636.67	11.25	1245291	110696	201	1615
2634.67	11.30	1283170	113598	207	1658
2632.67	11.34	1321050	116477	212	1700
2630.67	11.39	1358929	119333	217	1742
2628.67	11.43	1396809	122167	222	1783
2626.67	11.48	1434689	124978	227	1824
2624.67	11.53	1472568	127767	232	1865
2622.67	11.57	1510448	130533	237	1905
2620.67	11.62	1548327	133279	242	1945
2618.67	11.66	1586207	136002	247	1985
2616.67	11.71	1624086	138705	252	2024
2614.67	11.75	1661966	141387	257	2063

El. of Jet underside (ft)	Area of jet footprint (ft ²)	Stream power density (ft-lb/s/ft)	Stream power density (ft-lb/s-ft ²)	Stream power density (HP/ft ²)	Stream power density (kW/m ²)
2612.67	11.80	1699846	144048	262	2102
2610.67	11.85	1737725	146689	267	2141
2608.67	11.89	1775605	149309	271	2179
2606.67	11.94	1813484	151909	276	2217
2604.67	11.98	1851364	154490	281	2255
2602.67	12.03	1889243	157051	286	2292
2600.67	12.08	1927123	159593	290	2329
2598.67	12.12	1965003	162116	295	2366
2596.67	12.17	2002882	164620	299	2402
2594.67	12.21	2040762	167105	304	2439
2592.67	12.26	2078641	169572	308	2475
2590.67	12.30	2116521	172020	313	2510
2588.67	12.35	2154400	174451	317	2546
2586.67	12.40	2192280	176863	322	2581
2584.67	12.44	2230160	179258	326	2616
2582.67	12.49	2268039	181636	330	2651
2580.67	12.53	2305919	183996	335	2685
2578.67	12.58	2343798	186339	339	2719
2576.67	12.62	2381678	188665	343	2753
2574.67	12.67	2419557	190974	347	2787
2572.67	12.72	2457437	193267	351	2820
2570.67	12.76	2495316	195544	356	2854
2568.67	12.81	2533196	197804	360	2887
2566.67	12.85	2571076	200048	364	2919
2564.67	12.90	2608955	202277	368	2952
2562.67	12.94	2646835	204489	372	2984
2560.67	12.99	2684714	206687	376	3016
2558.67	13.03	2722594	208868	380	3048
2556.67	13.08	2760473	211035	384	3080
2554.67	13.13	2798353	213187	388	3111
2552.67	13.17	2836233	215323	391	3142
2550.67	13.22	2874112	217445	395	3173
2548.67	13.26	2911992	219553	399	3204
2546.67	13.31	2949871	221646	403	3235
2544.67	13.35	2987751	223724	407	3265
2542.67	13.40	3025630	225789	411	3295
2540.67	13.45	3063510	227840	414	3325
2538.67	13.49	3101390	229876	418	3355
2536.67	13.54	3139269	231899	422	3384
2534.67	13.58	3177149	233909	425	3414
2532.67	13.63	3215028	235905	429	3443
2531.00	13.67	3246658	237561	432	3467
2530.67	13.78	3252908	236009	429	3444
2528.67	14.49	3290787	227134	413	3315
2526.67	15.19	3328667	219083	398	3197
2524.67	15.90	3366547	211747	385	3090
2522.67	16.60	3404426	205034	373	2992
2520.67	17.31	3442306	198868	362	2902
2518.67	18.01	3480185	193184	351	2819
2516.67	18.72	3518065	187929	342	2743
2514.67	19.43	3555944	183056	333	2671

El. of Jet underside (ft)	Area of jet footprint (ft ²)	Stream power density (ft-lb/s/ft)	Stream power density (ft-lb/s-ft ²)	Stream power density (HP/ft ²)	Stream power density (kW/m ²)
2512.67	20.13	3593824	178524	325	2605
2510.67	20.84	3631703	174299	317	2544
2508.67	21.54	3669583	170350	310	2486
2506.67	22.25	3707463	166652	303	2432
2504.67	22.95	3745342	163182	297	2381
2502.67	23.66	3783222	159918	291	2334
2500.67	24.36	3821101	156843	285	2289
2498.67	25.07	3858981	153941	280	2247
2496.67	25.77	3896860	151198	275	2207
2494.67	26.48	3934740	148601	270	2169
2492.67	27.18	3972620	146139	266	2133
2490.67	27.89	4010499	143801	261	2099
2488.67	28.59	4048379	141579	257	2066
2486.67	29.30	4086258	139464	254	2035
2484.67	30.01	4124138	137448	250	2006
2482.67	30.71	4162017	135525	246	1978
2480.67	31.42	4199897	133688	243	1951
2478.67	32.12	4237777	131932	240	1925
2476.67	32.83	4275656	130251	237	1901
2474.67	33.53	4313536	128641	234	1877
2472.67	34.24	4351415	127097	231	1855
2470.67	34.94	4389295	125616	228	1833
2468.67	35.65	4427174	124193	226	1812
2466.67	36.35	4465054	122825	223	1792
2464.67	37.06	4502934	121510	221	1773
2462.67	37.76	4540813	120244	219	1755
2460.67	38.47	4578693	119024	216	1737
2458.67	39.17	4616572	117848	214	1720
2456.67	39.88	4654452	116713	212	1703
2454.67	40.58	4692331	115618	210	1687
2452.67	41.29	4730211	114561	208	1672
2450.67	42.00	4768090	113539	206	1657
2448.67	42.70	4805970	112550	205	1643
2446.67	43.41	4843850	111594	203	1629
2444.67	44.11	4881729	110669	201	1615
2442.67	44.82	4919609	109772	200	1602
2440.67	45.52	4957488	108903	198	1589
2438.67	46.23	4995368	108061	196	1577
2436.67	46.93	5033247	107244	195	1565
2434.67	47.64	5071127	106452	194	1554
2432.67	48.34	5109007	105682	192	1542
2430.67	49.05	5146886	104935	191	1531
2428.67	49.75	5184766	104209	189	1521
2426.67	50.46	5222645	103503	188	1510
2424.67	51.16	5260525	102816	187	1500
2422.67	51.87	5298404	102149	186	1491
2420.67	52.57	5336284	101499	185	1481
2418.67	53.28	5374164	100866	183	1472
2416.67	53.99	5412043	100250	182	1463
2414.67	54.69	5449923	99650	181	1454
2412.67	55.40	5487802	99065	180	1446

El. of Jet underside (ft)	Area of jet footprint (ft ²)	Stream power density (ft-lb/s/ft)	Stream power density (ft-lb/s-ft ²)	Stream power density (HP/ft ²)	Stream power density (kW/m ²)
2410.67	56.10	5525682	98494	179	1437
2408.67	56.81	5563561	97938	178	1429
2406.67	57.51	5601441	97396	177	1421
2404.67	58.22	5639321	96867	176	1414
2402.67	58.92	5677200	96350	175	1406
2400.67	59.63	5715080	95846	174	1399
2398.67	60.33	5752959	95353	173	1392
2396.67	61.04	5790839	94872	172	1385
2394.67	61.74	5828718	94401	172	1378
2392.67	62.45	5866598	93942	171	1371
2390.67	63.15	5904477	93493	170	1364
2388.67	63.86	5942357	93053	169	1358
2386.67	64.57	5980237	92623	168	1352
2384.67	65.27	6018116	92203	168	1346
2382.67	65.98	6055996	91791	167	1340
2380.67	66.68	6093875	91388	166	1334
2378.67	67.39	6131755	90994	165	1328
2376.67	68.09	6169634	90608	165	1322
2374.67	68.80	6207514	90229	164	1317
2372.67	69.50	6245394	89859	163	1311
2370.67	70.21	6283273	89496	163	1306
2368.67	70.91	6321153	89140	162	1301
2366.67	71.62	6359032	88791	161	1296
2364.67	72.32	6396912	88449	161	1291
2362.67	73.03	6434791	88113	160	1286

Shaded row indicates the location of the tailwater elevation at the PMF.

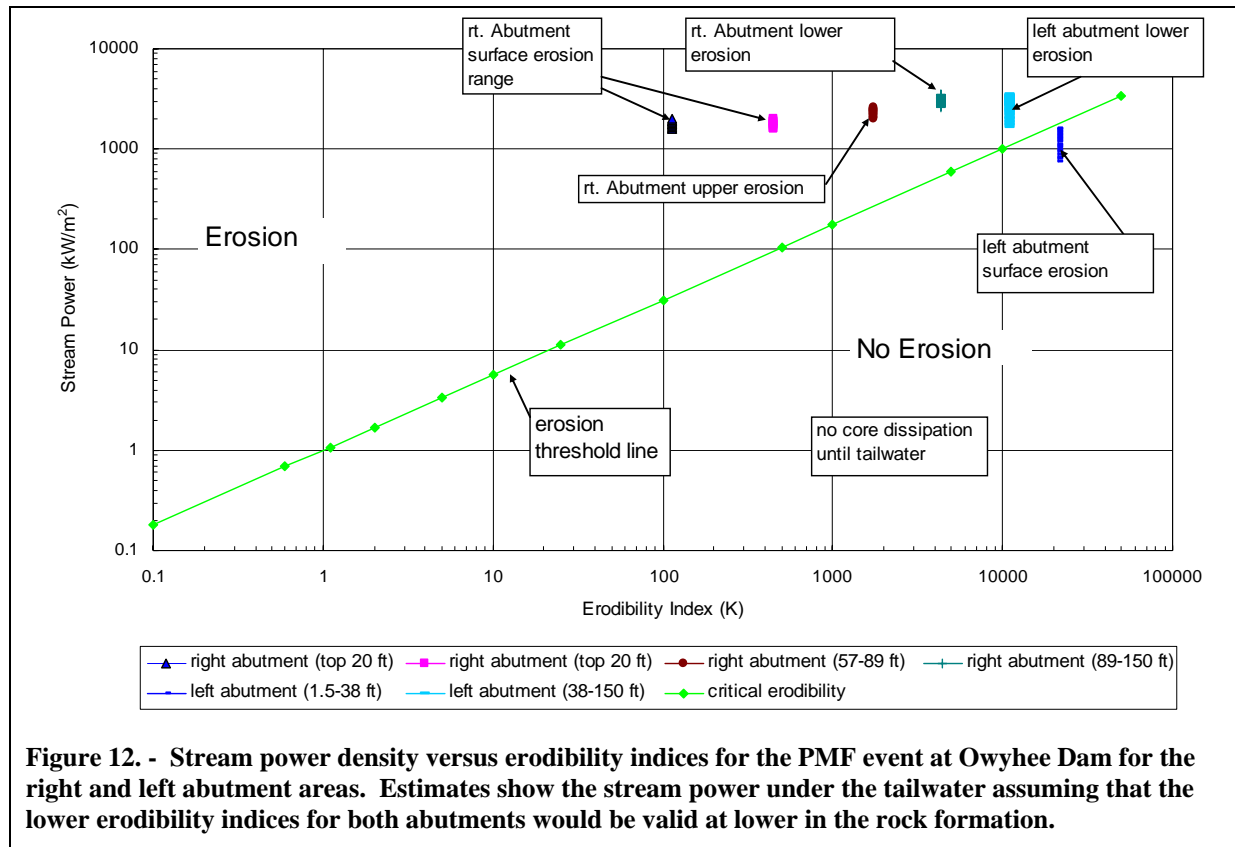


Figure 12 shows that the predicted stream power density under the PMF is large enough for erosion to be predicted for all of the various rock materials at all levels. The maximum stream power density of 432 HP/ft² or 3467 kW/m² occurs at the maximum drop from the dam to the abutments prior to the jet entering the tailwater pool. The right abutment surface rock below the gravity section is exposed to the lowest stream power, 1573 to 1985 kW/m², but the low erodibility index of the 20 ft of material still leads to the conclusion that erosion will occur. Underlying the tuff is stronger Rhyolite, for about 30 ft, but that material will be exposed to higher stream power densities of 2024 to 2581 kW/m² as the erosion hole forms from removal of the surface material. Stronger Rhyolite exists even further under the surface rock and would be exposed to stream power densities of 2516 kW/m² to the maximum if exposed. The left abutment area exposed to the flow is relatively small compared to the extent beneath the right abutment gravity dam. In this case, the surface rock is stronger than the lower rock but both would experience enough stream power to erode.

Conclusions

The following conclusions were drawn from analysis of the PMF flood event and potential erosion:

- The overtopping jet will impinge upon the rock abutments and into the tailwater at the toe of the dam.

- The jet will spread with potential decay of the core leading to break up of the jet after a certain free fall. The determination of the fall distance is not well known and conservative equations were used.
- The stream power density or erosive power of the jet per unit area was determined to vary from 647 to 3467 kW/m² over the various fall distances below Owyhee Dam.
- Examination of the chart for the erodibility index versus stream power for the PMF indicates that erosion is expected in all areas under the trajectory except deeper in the left abutment.
- There is quite a bit of uncertainty in the results due to the lack of research regarding rectangular free-falling jets and the lack of geological data at the dam site and how it might be applied to the erodibility index analysis.

Recommendations

The following recommendations are made as a result of this investigation into the hydraulic loading due to the PMF overtopping at Owyhee Dam:

- Investigate whether the right abutment gravity section would be stable with loss of a significant quantity of rock do to erosion during overtopping were to occur.
- Investigate if the rock cover over the spillway tunnel would be adequate if some rock erodes above the tunnel.
- Perform a risk analysis that might determine if the abutments would be stable under lesser flood events using the information in the appendix on the predicted stream power for other flood events.

In addition, it is recommended that further research be conducted on the properties of rectangular free-falling jets and rock characterization using the erodibility index. This would greatly enhance the reliability of further overtopping studies.

Acknowledgments

This project was requested by John Baals, Manager, Structural Analysis Group, 86-68110, to assist with the Corrective Action Study for Owyhee Dam. Joseph Kottenstette, Geotechnical Engineer, Geotechnical Engineering Group 2, 86-68132, provided the erodibility indices of the rock below the dam. Mark Steers, Civil Engineer, Waterways and Concrete Dams, 86-68130, provided the flood routing information. Bruce Feinberg, Hydraulic Engineer, Sedimentation and River Hydraulics Group, 86-68540, provided the estimates of the tailwater rating below the dam. Rudy Campbell, Water Resources Research Laboratory, 86-68560, provided assistance with the ACAD presentation of the results. Technical peer review was provided by Joseph Kubitschek, Hydraulic Engineer, Water Resources Research Laboratory, 86-68560.

References

- [1] "Geologic Report - Mapping Program - Safety Evaluation of Existing Dams - Owyhee Dam, Owyhee Project, Oregon," by Steve Acree and Karl Wirkus, Pacific Northwest Region, Bureau of Reclamation, January, 1982.
- [2] "Summary Geologic Report for Modification Decision Analysis - Safety of Dams Program - Owyhee Dam, Owyhee Project, Oregon," Bureau of Reclamation, Pacific Northwest Region, July 1991.
- [3] "Owyhee Dam Flood Routing Frequency Flood Routings," Owyhee Project, Oregon, Pacific Northwest Region, Technical Memorandum No. OWY-8130-CFR-2006-1, Technical Services Center, Bureau of Reclamation, Denver, Colorado, June 2006.
- [4] Notes by Bruce Feinberg, 86-68540, providing tailwater information.
- [5] Chow, Ven Te, "Open-Channel Hydraulic," McGraw-Hill, Inc., 1959.
- [6] Rouse, H. R., 1936, "Discharge Characteristics of the Free Overfall," Civil Engineering, Vol. 6, No. 4.
- [7] Bollaert, Erik, 2002, "Transient water pressures in joints and formation of rock scour due to high-velocity jet impact," Communication 13, Laboratoire de Constructions Hydrauliques Ecole Polytechnique Federale de Lausanne, Edited by Professor Dr. A. Schleiss, Lausanne, Switzerland, 2002.
- [8] Annandale, George W., 2006, "Scour Technology *Mechanics and Engineering Practice*," McGraw-Hill Civil Engineering Series, ISBN 0-07-144057-7.
- [9] Ervine and Falvey, 1987, "Behaviour of turbulent water jets in the atmosphere and in plunge pools," Proceedings Institution of Civil Engineers, Part 2, Volume 83, pp. 295-314.
- [10] Ervine, D.A., et al, 1997, "Pressure Fluctuations on Plunge Pool Floors," Journal of Hydraulic Research, Vol. 35, No. 2, pp. 257-279.

Appendix

Jet Trajectory Tables and Erodibility Plots for Events other than the PMF.

Table 8. - Trajectory locations for various frequency flood events with x (horizontal) and y (vertical) distances and elevations from the downstream parapet location. The elevation of the lower nappe, not the x distance, is always the same; therefore, not shown except for the 5,000 year event.

select y	5,000			10,000		20,000		50,000		1,000,000		10,000,000	
	x	el. Lower	el. Upper	x	el. Upper	x	el. Upper	x	el. Upper	x	el. Upper	x	el. Upper
0.00	0.00	2678.67	2679.72	0.00	2683.47	0.00	2681.63	0.00	2682.81	0.00	2683.71	0.00	2686.90
-2.00	3.39	2676.67	2677.72	4.73	2681.47	5.69	2679.63	6.73	2680.81	7.43	2681.71	9.49	2684.90
-4.00	4.80	2674.67	2675.72	6.70	2679.47	8.05	2677.63	9.52	2678.81	10.51	2679.71	13.43	2682.90
-6.00	5.88	2672.67	2673.72	8.20	2677.47	9.86	2675.63	11.66	2676.81	12.87	2677.71	16.44	2680.90
-8.00	6.79	2670.67	2671.72	9.47	2675.47	11.39	2673.63	13.46	2674.81	14.86	2675.71	18.99	2678.90
-10.00	7.59	2668.67	2669.72	10.59	2673.47	12.73	2671.63	15.05	2672.81	16.61	2673.71	21.23	2676.90
-12.00	8.31	2666.67	2667.72	11.60	2671.47	13.95	2669.63	16.49	2670.81	18.20	2671.71	23.25	2674.90
-14.00	8.98	2664.67	2665.72	12.53	2669.47	15.06	2667.63	17.81	2668.81	19.66	2669.71	25.12	2672.90
-16.00	9.60	2662.67	2663.72	13.39	2667.47	16.10	2665.63	19.04	2666.81	21.01	2667.71	26.85	2670.90
-18.00	10.18	2660.67	2661.72	14.20	2665.47	17.08	2663.63	20.19	2664.81	22.29	2665.71	28.48	2668.90
-20.00	10.73	2658.67	2659.72	14.97	2663.47	18.01	2661.63	21.29	2662.81	23.49	2663.71	30.02	2666.90
-22.00	11.26	2656.67	2657.72	15.70	2661.47	18.88	2659.63	22.33	2660.81	24.64	2661.71	31.48	2664.90
-24.00	11.76	2654.67	2655.72	16.40	2659.47	19.72	2657.63	23.32	2658.81	25.74	2659.71	32.88	2662.90
-26.00	12.24	2652.67	2653.72	17.07	2657.47	20.53	2655.63	24.27	2656.81	26.79	2657.71	34.23	2660.90
-28.00	12.70	2650.67	2651.72	17.71	2655.47	21.30	2653.63	25.19	2654.81	27.80	2655.71	35.52	2658.90
-30.00	13.14	2648.67	2649.72	18.34	2653.47	22.05	2651.63	26.07	2652.81	28.77	2653.71	36.77	2656.90
-32.00	13.57	2646.67	2647.72	18.94	2651.47	22.78	2649.63	26.93	2650.81	29.72	2651.71	37.97	2654.90
-34.00	13.99	2644.67	2645.72	19.52	2649.47	23.48	2647.63	27.75	2648.81	30.63	2649.71	39.14	2652.90
-36.00	14.40	2642.67	2643.72	20.09	2647.47	24.16	2645.63	28.56	2646.81	31.52	2647.71	40.28	2650.90
-38.00	14.79	2640.67	2641.72	20.64	2645.47	24.82	2643.63	29.34	2644.81	32.39	2645.71	41.38	2648.90
-40.00	15.18	2638.67	2639.72	21.17	2643.47	25.46	2641.63	30.10	2642.81	33.23	2643.71	42.45	2646.90
-42.00	15.55	2636.67	2637.72	21.70	2641.47	26.09	2639.63	30.85	2640.81	34.05	2641.71	43.50	2644.90
-44.00	15.92	2634.67	2635.72	22.21	2639.47	26.71	2637.63	31.57	2638.81	34.85	2639.71	44.53	2642.90
-46.00	16.28	2632.67	2633.72	22.71	2637.47	27.31	2635.63	32.28	2636.81	35.63	2637.71	45.53	2640.90
-48.00	16.63	2630.67	2631.72	23.19	2635.47	27.89	2633.63	32.98	2634.81	36.40	2635.71	46.51	2638.90
-50.00	16.97	2628.67	2629.72	23.67	2633.47	28.47	2631.63	33.66	2632.81	37.15	2633.71	47.46	2636.90
-52.00	17.30	2626.67	2627.72	24.14	2631.47	29.03	2629.63	34.32	2630.81	37.88	2631.71	48.40	2634.90
-54.00	17.63	2624.67	2625.72	24.60	2629.47	29.59	2627.63	34.98	2628.81	38.61	2629.71	49.33	2632.90
-56.00	17.96	2622.67	2623.72	25.05	2627.47	30.13	2625.63	35.62	2626.81	39.31	2627.71	50.23	2630.90
-58.00	18.28	2620.67	2621.72	25.50	2625.47	30.66	2623.63	36.25	2624.81	40.01	2625.71	51.12	2628.90
-60.00	18.59	2618.67	2619.72	25.93	2623.47	31.19	2621.63	36.87	2622.81	40.69	2623.71	51.99	2626.90
-62.00	18.89	2616.67	2617.72	26.36	2621.47	31.70	2619.63	37.48	2620.81	41.37	2621.71	52.85	2624.90
-64.00	19.20	2614.67	2615.72	26.78	2619.47	32.21	2617.63	38.08	2618.81	42.03	2619.71	53.70	2622.90
-66.00	19.49	2612.67	2613.72	27.20	2617.47	32.71	2615.63	38.67	2616.81	42.68	2617.71	54.53	2620.90
-68.00	19.79	2610.67	2611.72	27.61	2615.47	33.20	2613.63	39.25	2614.81	43.32	2615.71	55.35	2618.90
-70.00	20.08	2608.67	2609.72	28.01	2613.47	33.68	2611.63	39.82	2612.81	43.95	2613.71	56.16	2616.90
-72.00	20.36	2606.67	2607.72	28.41	2611.47	34.16	2609.63	40.39	2610.81	44.58	2611.71	56.96	2614.90
-74.00	20.64	2604.67	2605.72	28.80	2609.47	34.63	2607.63	40.94	2608.81	45.19	2609.71	57.74	2612.90
-76.00	20.92	2602.67	2603.72	29.18	2607.47	35.10	2605.63	41.49	2606.81	45.80	2607.71	58.52	2610.90
-78.00	21.19	2600.67	2601.72	29.57	2605.47	35.56	2603.63	42.04	2604.81	46.40	2605.71	59.28	2608.90
-80.00	21.46	2598.67	2599.72	29.94	2603.47	36.01	2601.63	42.57	2602.81	46.99	2603.71	60.04	2606.90
-82.00	21.73	2596.67	2597.72	30.31	2601.47	36.46	2599.63	43.10	2600.81	47.57	2601.71	60.78	2604.90
-84.00	21.99	2594.67	2595.72	30.68	2599.47	36.90	2597.63	43.62	2598.81	48.15	2599.71	61.52	2602.90
-86.00	22.25	2592.67	2593.72	31.05	2597.47	37.34	2595.63	44.14	2596.81	48.72	2597.71	62.25	2600.90
-88.00	22.51	2590.67	2591.72	31.40	2595.47	37.77	2593.63	44.65	2594.81	49.28	2595.71	62.97	2598.90

select y	5,000			10,000		20,000		50,000		1,000,000		10,000,000	
	x	el. Lower	el. Upper	x	el. Upper	x	el. Upper	x	el. Upper	x	el. Upper	x	el. Upper
-90.00	22.77	2588.67	2589.72	31.76	2593.47	38.19	2591.63	45.15	2592.81	49.84	2593.71	63.68	2596.90
-92.00	23.02	2586.67	2587.72	32.11	2591.47	38.62	2589.63	45.65	2590.81	50.39	2591.71	64.38	2594.90
-94.00	23.27	2584.67	2585.72	32.46	2589.47	39.03	2587.63	46.15	2588.81	50.94	2589.71	65.08	2592.90
-96.00	23.51	2582.67	2583.72	32.80	2587.47	39.45	2585.63	46.64	2586.81	51.47	2587.71	65.77	2590.90
-98.00	23.76	2580.67	2581.72	33.14	2585.47	39.86	2583.63	47.12	2584.81	52.01	2585.71	66.45	2588.90
-100.00	24.00	2578.67	2579.72	33.48	2583.47	40.26	2581.63	47.60	2582.81	52.54	2583.71	67.13	2586.90
-102.00	24.24	2576.67	2577.72	33.81	2581.47	40.66	2579.63	48.07	2580.81	53.06	2581.71	67.79	2584.90
-104.00	24.47	2574.67	2575.72	34.14	2579.47	41.06	2577.63	48.54	2578.81	53.58	2579.71	68.45	2582.90
-106.00	24.71	2572.67	2573.72	34.47	2577.47	41.45	2575.63	49.00	2576.81	54.09	2577.71	69.11	2580.90
-108.00	24.94	2570.67	2571.72	34.79	2575.47	41.84	2573.63	49.46	2574.81	54.60	2575.71	69.76	2578.90
-110.00	25.17	2568.67	2569.72	35.11	2573.47	42.23	2571.63	49.92	2572.81	55.10	2573.71	70.40	2576.90
-112.00	25.40	2566.67	2567.72	35.43	2571.47	42.61	2569.63	50.37	2570.81	55.60	2571.71	71.04	2574.90
-114.00	25.62	2564.67	2565.72	35.74	2569.47	42.99	2567.63	50.82	2568.81	56.09	2569.71	71.67	2572.90
-116.00	25.85	2562.67	2563.72	36.06	2567.47	43.36	2565.63	51.26	2566.81	56.58	2567.71	72.30	2570.90
-118.00	26.07	2560.67	2561.72	36.37	2565.47	43.73	2563.63	51.70	2564.81	57.07	2565.71	72.92	2568.90
-120.00	26.29	2558.67	2559.72	36.67	2563.47	44.10	2561.63	52.14	2562.81	57.55	2563.71	73.53	2566.90
-122.00	26.51	2556.67	2557.72	36.98	2561.47	44.47	2559.63	52.57	2560.81	58.03	2561.71	74.14	2564.90
-124.00	26.72	2554.67	2555.72	37.28	2559.47	44.83	2557.63	53.00	2558.81	58.50	2559.71	74.75	2562.90
-126.00	26.94	2552.67	2553.72	37.58	2557.47	45.19	2555.63	53.43	2556.81	58.97	2557.71	75.35	2560.90
-128.00	27.15	2550.67	2551.72	37.88	2555.47	45.55	2553.63	53.85	2554.81	59.44	2555.71	75.94	2558.90
-130.00	27.36	2548.67	2549.72	38.17	2553.47	45.90	2551.63	54.27	2552.81	59.90	2553.71	76.53	2556.90
-132.00	27.57	2546.67	2547.72	38.46	2551.47	46.26	2549.63	54.69	2550.81	60.36	2551.71	77.12	2554.90
-134.00	27.78	2544.67	2545.72	38.75	2549.47	46.61	2547.63	55.10	2548.81	60.81	2549.71	77.70	2552.90
-136.00	27.98	2542.67	2543.72	39.04	2547.47	46.95	2545.63	55.51	2546.81	61.27	2547.71	78.28	2550.90
-138.00	28.19	2540.67	2541.72	39.33	2545.47	47.30	2543.63	55.91	2544.81	61.72	2545.71	78.85	2548.90
-140.00	28.39	2538.67	2539.72	39.61	2543.47	47.64	2541.63	56.32	2542.81	62.16	2543.71	79.42	2546.90
-142.00	28.60	2536.67	2537.72	39.89	2541.47	47.98	2539.63	56.72	2540.81	62.60	2541.71	79.99	2544.90
-144.00	28.80	2534.67	2535.72	40.17	2539.47	48.31	2537.63	57.12	2538.81	63.04	2539.71	80.55	2542.90
-146.00	29.00	2532.67	2533.72	40.45	2537.47	48.65	2535.63	57.51	2536.81	63.48	2537.71	81.11	2540.90
-147.67	29.16	2531.00	2532.05	40.68	2535.80	48.92	2533.96	57.84	2535.14	63.84	2536.04	81.57	2539.23
-148.00	29.19	2530.67	2531.72	40.73	2535.47	48.98	2533.63	57.90	2534.81	63.91	2535.71	81.66	2538.90
-150.00	29.39	2528.67	2529.72	41.00	2533.47	49.31	2531.63	58.29	2532.81	64.34	2533.71	82.21	2536.90
-152.00	29.59	2526.67	2527.72	41.27	2531.47	49.64	2529.63	58.68	2530.81	64.77	2531.71	82.76	2534.90
-154.00	29.78	2524.67	2525.72	41.54	2529.47	49.96	2527.63	59.07	2528.81	65.19	2529.71	83.30	2532.90
-156.00	29.97	2522.67	2523.72	41.81	2527.47	50.29	2525.63	59.45	2526.81	65.62	2527.71	83.84	2530.90
-158.00	30.16	2520.67	2521.72	42.08	2525.47	50.61	2523.63	59.83	2524.81	66.04	2525.71	84.37	2528.90
-160.00	30.35	2518.67	2519.72	42.35	2523.47	50.93	2521.63	60.21	2522.81	66.45	2523.71	84.91	2526.90
-162.00	30.54	2516.67	2517.72	42.61	2521.47	51.24	2519.63	60.58	2520.81	66.87	2521.71	85.44	2524.90
-164.00	30.73	2514.67	2515.72	42.87	2519.47	51.56	2517.63	60.95	2518.81	67.28	2519.71	85.96	2522.90
-166.00	30.92	2512.67	2513.72	43.13	2517.47	51.87	2515.63	61.32	2516.81	67.69	2517.71	86.48	2520.90
-168.00	31.10	2510.67	2511.72	43.39	2515.47	52.18	2513.63	61.69	2514.81	68.09	2515.71	87.00	2518.90
-170.00	31.29	2508.67	2509.72	43.65	2513.47	52.49	2511.63	62.06	2512.81	68.50	2513.71	87.52	2516.90
-172.00	31.47	2506.67	2507.72	43.90	2511.47	52.80	2509.63	62.42	2510.81	68.90	2511.71	88.03	2514.90
-174.00	31.65	2504.67	2505.72	44.16	2509.47	53.11	2507.63	62.79	2508.81	69.30	2509.71	88.54	2512.90
-176.00	31.84	2502.67	2503.72	44.41	2507.47	53.41	2505.63	63.14	2506.81	69.70	2507.71	89.05	2510.90
-178.00	32.02	2500.67	2501.72	44.66	2505.47	53.71	2503.63	63.50	2504.81	70.09	2505.71	89.56	2508.90
-180.00	32.19	2498.67	2499.72	44.91	2503.47	54.02	2501.63	63.86	2502.81	70.48	2503.71	90.06	2506.90
-182.00	32.37	2496.67	2497.72	45.16	2501.47	54.32	2499.63	64.21	2500.81	70.87	2501.71	90.56	2504.90
-184.00	32.55	2494.67	2495.72	45.41	2499.47	54.61	2497.63	64.56	2498.81	71.26	2499.71	91.05	2502.90
-186.00	32.73	2492.67	2493.72	45.66	2497.47	54.91	2495.63	64.91	2496.81	71.65	2497.71	91.55	2500.90
-188.00	32.90	2490.67	2491.72	45.90	2495.47	55.20	2493.63	65.26	2494.81	72.03	2495.71	92.04	2498.90
-190.00	33.08	2488.67	2489.72	46.15	2493.47	55.50	2491.63	65.61	2492.81	72.42	2493.71	92.53	2496.90

select y	5,000			10,000		20,000		50,000		1,000,000		10,000,000	
	x	el. Lower	el. Upper	x	el. Upper	x	el. Upper	x	el. Upper	x	el. Upper	x	el. Upper
-192.00	33.25	2486.67	2487.72	46.39	2491.47	55.79	2489.63	65.95	2490.81	72.80	2491.71	93.01	2494.90
-194.00	33.42	2484.67	2485.72	46.63	2489.47	56.08	2487.63	66.30	2488.81	73.17	2489.71	93.49	2492.90
-196.00	33.60	2482.67	2483.72	46.87	2487.47	56.37	2485.63	66.64	2486.81	73.55	2487.71	93.98	2490.90
-198.00	33.77	2480.67	2481.72	47.11	2485.47	56.65	2483.63	66.98	2484.81	73.92	2485.71	94.45	2488.90
-200.00	33.94	2478.67	2479.72	47.34	2483.47	56.94	2481.63	67.31	2482.81	74.30	2483.71	94.93	2486.90
-202.00	34.11	2476.67	2477.72	47.58	2481.47	57.22	2479.63	67.65	2480.81	74.67	2481.71	95.40	2484.90
-204.00	34.27	2474.67	2475.72	47.81	2479.47	57.50	2477.63	67.98	2478.81	75.04	2479.71	95.87	2482.90
-206.00	34.44	2472.67	2473.72	48.05	2477.47	57.79	2475.63	68.31	2476.81	75.40	2477.71	96.34	2480.90
-208.00	34.61	2470.67	2471.72	48.28	2475.47	58.07	2473.63	68.65	2474.81	75.77	2475.71	96.81	2478.90
-210.00	34.77	2468.67	2469.72	48.51	2473.47	58.34	2471.63	68.98	2472.81	76.13	2473.71	97.27	2476.90
-212.00	34.94	2466.67	2467.72	48.74	2471.47	58.62	2469.63	69.30	2470.81	76.49	2471.71	97.74	2474.90
-214.00	35.10	2464.67	2465.72	48.97	2469.47	58.90	2467.63	69.63	2468.81	76.85	2469.71	98.20	2472.90
-216.00	35.27	2462.67	2463.72	49.20	2467.47	59.17	2465.63	69.95	2466.81	77.21	2467.71	98.65	2470.90
-218.00	35.43	2460.67	2461.72	49.43	2465.47	59.44	2463.63	70.28	2464.81	77.57	2465.71	99.11	2468.90
-220.00	35.59	2458.67	2459.72	49.65	2463.47	59.72	2461.63	70.60	2462.81	77.92	2463.71	99.56	2466.90
-222.00	35.75	2456.67	2457.72	49.88	2461.47	59.99	2459.63	70.92	2460.81	78.28	2461.71	100.01	2464.90
-224.00	35.91	2454.67	2455.72	50.10	2459.47	60.26	2457.63	71.24	2458.81	78.63	2459.71	100.46	2462.90
-226.00	36.07	2452.67	2453.72	50.33	2457.47	60.53	2455.63	71.55	2456.81	78.98	2457.71	100.91	2460.90
-228.00	36.23	2450.67	2451.72	50.55	2455.47	60.79	2453.63	71.87	2454.81	79.33	2455.71	101.36	2458.90
-230.00	36.39	2448.67	2449.72	50.77	2453.47	61.06	2451.63	72.18	2452.81	79.67	2453.71	101.80	2456.90
-232.00	36.55	2446.67	2447.72	50.99	2451.47	61.32	2449.63	72.50	2450.81	80.02	2451.71	102.24	2454.90
-234.00	36.71	2444.67	2445.72	51.21	2449.47	61.59	2447.63	72.81	2448.81	80.36	2449.71	102.68	2452.90
-236.00	36.86	2442.67	2443.72	51.43	2447.47	61.85	2445.63	73.12	2446.81	80.71	2447.71	103.12	2450.90
-238.00	37.02	2440.67	2441.72	51.65	2445.47	62.11	2443.63	73.43	2444.81	81.05	2445.71	103.56	2448.90
-240.00	37.18	2438.67	2439.72	51.86	2443.47	62.37	2441.63	73.74	2442.81	81.39	2443.71	103.99	2446.90
-242.00	37.33	2436.67	2437.72	52.08	2441.47	62.63	2439.63	74.04	2440.81	81.73	2441.71	104.42	2444.90
-244.00	37.48	2434.67	2435.72	52.29	2439.47	62.89	2437.63	74.35	2438.81	82.06	2439.71	104.85	2442.90
-246.00	37.64	2432.67	2433.72	52.51	2437.47	63.15	2435.63	74.65	2436.81	82.40	2437.71	105.28	2440.90
-248.00	37.79	2430.67	2431.72	52.72	2435.47	63.40	2433.63	74.96	2434.81	82.73	2435.71	105.71	2438.90
-250.00	37.94	2428.67	2429.72	52.93	2433.47	63.66	2431.63	75.26	2432.81	83.07	2433.71	106.13	2436.90
-252.00	38.09	2426.67	2427.72	53.14	2431.47	63.91	2429.63	75.56	2430.81	83.40	2431.71	106.56	2434.90
-254.00	38.24	2424.67	2425.72	53.35	2429.47	64.17	2427.63	75.86	2428.81	83.73	2429.71	106.98	2432.90
-256.00	38.39	2422.67	2423.72	53.56	2427.47	64.42	2425.63	76.16	2426.81	84.06	2427.71	107.40	2430.90
-258.00	38.54	2420.67	2421.72	53.77	2425.47	64.67	2423.63	76.45	2424.81	84.38	2425.71	107.82	2428.90
-260.00	38.69	2418.67	2419.72	53.98	2423.47	64.92	2421.63	76.75	2422.81	84.71	2423.71	108.24	2426.90
-262.00	38.84	2416.67	2417.72	54.19	2421.47	65.17	2419.63	77.04	2420.81	85.04	2421.71	108.65	2424.90
-264.00	38.99	2414.67	2415.72	54.39	2419.47	65.42	2417.63	77.34	2418.81	85.36	2419.71	109.07	2422.90
-266.00	39.14	2412.67	2413.72	54.60	2417.47	65.66	2415.63	77.63	2416.81	85.68	2417.71	109.48	2420.90
-268.00	39.28	2410.67	2411.72	54.80	2415.47	65.91	2413.63	77.92	2414.81	86.00	2415.71	109.89	2418.90
-270.00	39.43	2408.67	2409.72	55.01	2413.47	66.16	2411.63	78.21	2412.81	86.32	2413.71	110.30	2416.90
-272.00	39.58	2406.67	2407.72	55.21	2411.47	66.40	2409.63	78.50	2410.81	86.64	2411.71	110.71	2414.90
-274.00	39.72	2404.67	2405.72	55.41	2409.47	66.64	2407.63	78.79	2408.81	86.96	2409.71	111.11	2412.90
-276.00	39.87	2402.67	2403.72	55.62	2407.47	66.89	2405.63	79.07	2406.81	87.28	2407.71	111.52	2410.90
-278.00	40.01	2400.67	2401.72	55.82	2405.47	67.13	2403.63	79.36	2404.81	87.59	2405.71	111.92	2408.90
-280.00	40.15	2398.67	2399.72	56.02	2403.47	67.37	2401.63	79.65	2402.81	87.91	2403.71	112.32	2406.90
-282.00	40.30	2396.67	2397.72	56.22	2401.47	67.61	2399.63	79.93	2400.81	88.22	2401.71	112.72	2404.90
-284.00	40.44	2394.67	2395.72	56.42	2399.47	67.85	2397.63	80.21	2398.81	88.53	2399.71	113.12	2402.90
-286.00	40.58	2392.67	2393.72	56.62	2397.47	68.09	2395.63	80.49	2396.81	88.85	2397.71	113.52	2400.90
-288.00	40.72	2390.67	2391.72	56.81	2395.47	68.33	2393.63	80.78	2394.81	89.16	2395.71	113.92	2398.90
-290.00	40.86	2388.67	2389.72	57.01	2393.47	68.56	2391.63	81.06	2392.81	89.46	2393.71	114.31	2396.90
-292.00	41.01	2386.67	2387.72	57.21	2391.47	68.80	2389.63	81.33	2390.81	89.77	2391.71	114.70	2394.90
-294.00	41.15	2384.67	2385.72	57.40	2389.47	69.03	2387.63	81.61	2388.81	90.08	2389.71	115.10	2392.90

select y	5,000			10,000		20,000		50,000		1,000,000		10,000,000	
	x	el. Lower	el. Upper	x	el. Upper	x	el. Upper	x	el. Upper	x	el. Upper	x	el. Upper
-296.00	41.29	2382.67	2383.72	57.60	2387.47	69.27	2385.63	81.89	2386.81	90.39	2387.71	115.49	2390.90
-298.00	41.42	2380.67	2381.72	57.79	2385.47	69.50	2383.63	82.17	2384.81	90.69	2385.71	115.88	2388.90
-300.00	41.56	2378.67	2379.72	57.98	2383.47	69.73	2381.63	82.44	2382.81	90.99	2383.71	116.26	2386.90
-302.00	41.70	2376.67	2377.72	58.18	2381.47	69.97	2379.63	82.72	2380.81	91.30	2381.71	116.65	2384.90
-304.00	41.84	2374.67	2375.72	58.37	2379.47	70.20	2377.63	82.99	2378.81	91.60	2379.71	117.04	2382.90
-306.00	41.98	2372.67	2373.72	58.56	2377.47	70.43	2375.63	83.26	2376.81	91.90	2377.71	117.42	2380.90
-308.00	42.11	2370.67	2371.72	58.75	2375.47	70.66	2373.63	83.53	2374.81	92.20	2375.71	117.80	2378.90
-310.00	42.25	2368.67	2369.72	58.94	2373.47	70.89	2371.63	83.80	2372.81	92.50	2373.71	118.19	2376.90
-312.00	42.39	2366.67	2367.72	59.13	2371.47	71.12	2369.63	84.07	2370.81	92.80	2371.71	118.57	2374.90
-314.00	42.52	2364.67	2365.72	59.32	2369.47	71.34	2367.63	84.34	2368.81	93.09	2369.71	118.95	2372.90
-316.00	42.66	2362.67	2363.72	59.51	2367.47	71.57	2365.63	84.61	2366.81	93.39	2367.71	119.32	2370.90
-318.00	42.79	2360.67	2361.72	59.70	2365.47	71.80	2363.63	84.88	2364.81	93.68	2365.71	119.70	2368.90
-320.00	42.93	2358.67	2359.72	59.89	2363.47	72.02	2361.63	85.14	2362.81	93.98	2363.71	120.08	2366.90
-322.00	43.06	2356.67	2357.72	60.07	2361.47	72.25	2359.63	85.41	2360.81	94.27	2361.71	120.45	2364.90
-324.00	43.19	2354.67	2355.72	60.26	2359.47	72.47	2357.63	85.68	2358.81	94.56	2359.71	120.83	2362.90
-326.00	43.33	2352.67	2353.72	60.44	2357.47	72.69	2355.63	85.94	2356.81	94.86	2357.71	121.20	2360.90
-328.00	43.46	2350.67	2351.72	60.63	2355.47	72.92	2353.63	86.20	2354.81	95.15	2355.71	121.57	2358.90
-330.00	43.59	2348.67	2349.72	60.81	2353.47	73.14	2351.63	86.46	2352.81	95.44	2353.71	121.94	2356.90

Figures 1A-6A shows the stream power density resulting from additional calculations for the flood events of 5,000 to 1,000,000-year frequencies.

The core of the jet will break up after a certain fall distance. Using the conservative equation of $L_b = 50-100t$, the jet is broken up for the following events at the elevations given in table 1A. The core of the jet will break up while falling through the air for flood events of 50,000 years and below. This means no additional impact below that point, but still stream power of associated with the fall of the water mass and the footprint of the area.

Table 1A. - Fall distances of the jet to predicted break up.

Flood frequency (years)	Fall distance below crest to jet break up (ft)	El. Below crest of fall distance to jet break up (ft)	Tailwater El. (ft)	Comments
10M (PMF)	507	2171.67	2531	Still energy below tw
1M	411	2267.67	2514	Still energy below tw
100k	252	2426.67	2482	Still energy below tw
50k	208	2470.67	2473	Core dissipates at same elevation as tw
20k	148	2530.67	2461	Core dissipates 30 ft above the

Flood frequency (years)	Fall distance below crest to jet break up (ft)	El. Below crest of fall distance to jet break up (ft)	Tailwater El. (ft)	Comments
				tw
10k	102	2581.47	2451	Core dissipates 30 ft above the tw
5k	53	2624.67	2443	Jet break up 181 ft above the tw

The result of the erodibility study is that erosion will still occur for all flood frequencies because the rock condition is poor on high up on the right abutment below the gravity dam. The rock quality is better lower in the rock, but the erosive power is great enough to cause predicted erosion until a flood frequency of 10,000 years and below is reached. The material lower on the left abutment has less strength than the material higher up on the abutment and is predicted to erode if exposed. The material higher up on the left abutment is predicted to not erode, however; even under the PMF.

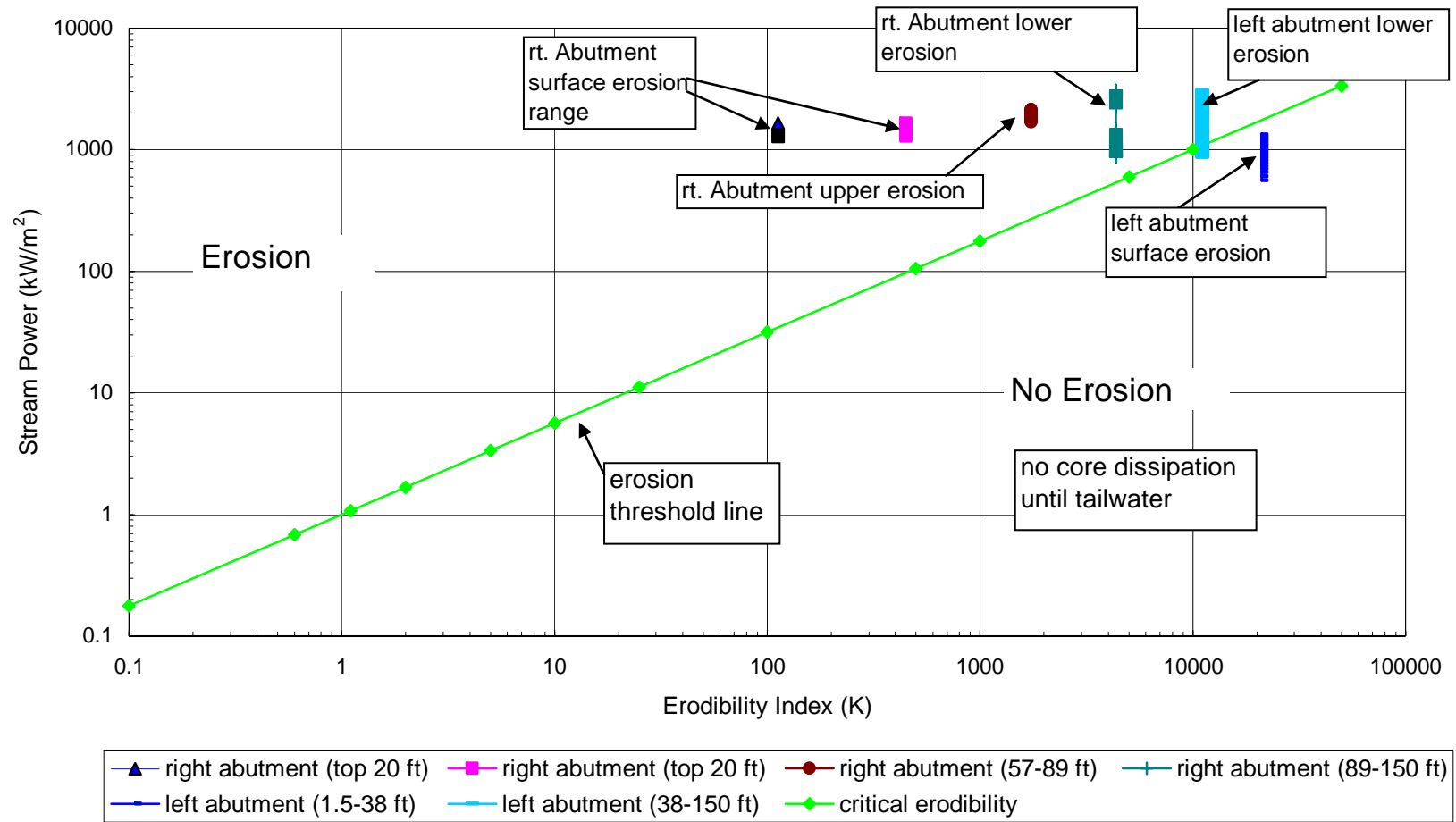


Figure 1A. - 1,000,000-year flood event. Core will not dissipate in the free fall. Below the tailwater it will dissipate, thus not adding additional pressure fluctuations, but stream power will still develop to the footprint of the spread of the jet.

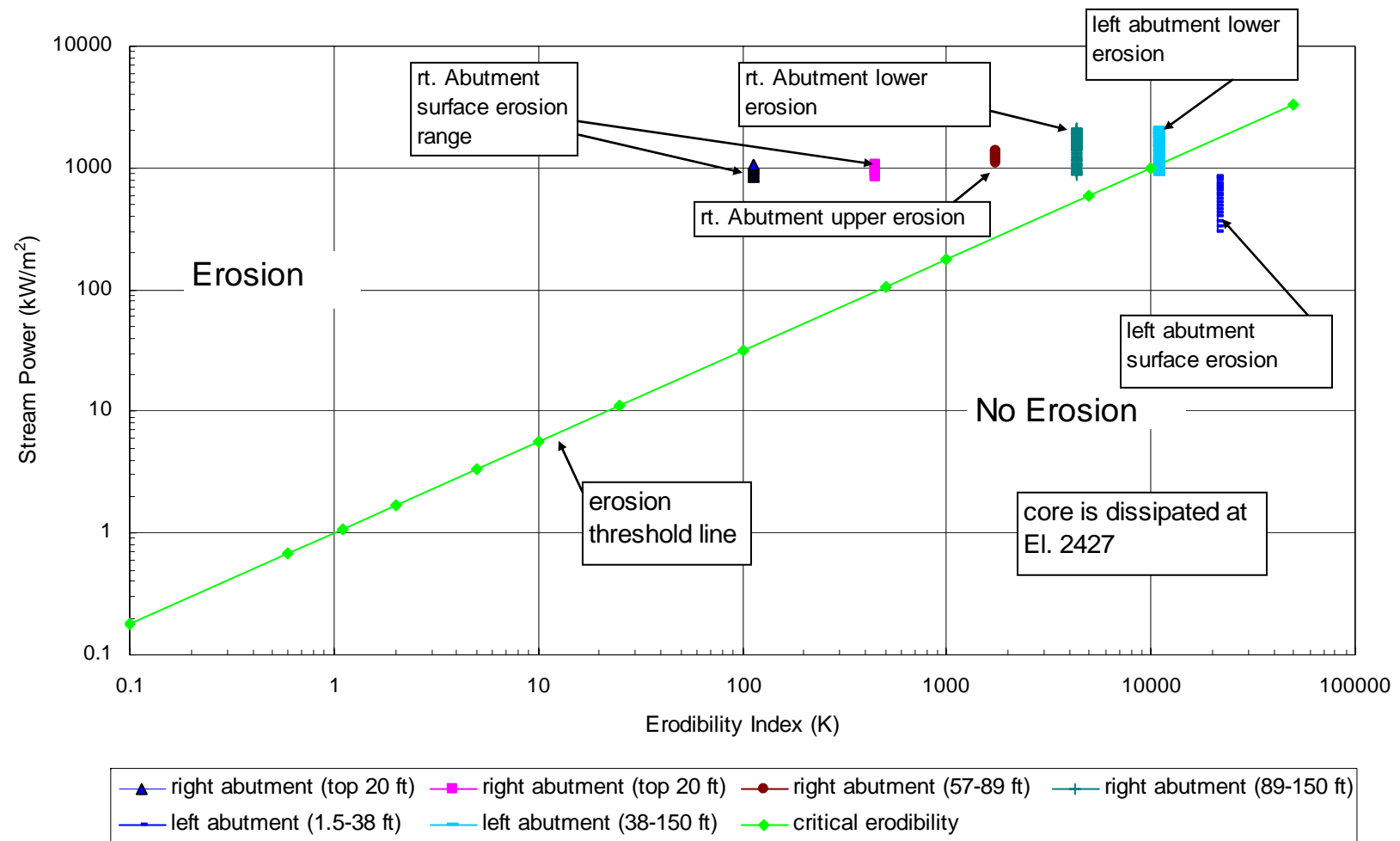


Figure 2A. - 100,000-yr flood event. Core dissipates at El. 2427 or about 55 ft below the tailwater. The core will dissipate in the tailwater, thus not adding pressure fluctuations to the impact, but still stream power will exist.

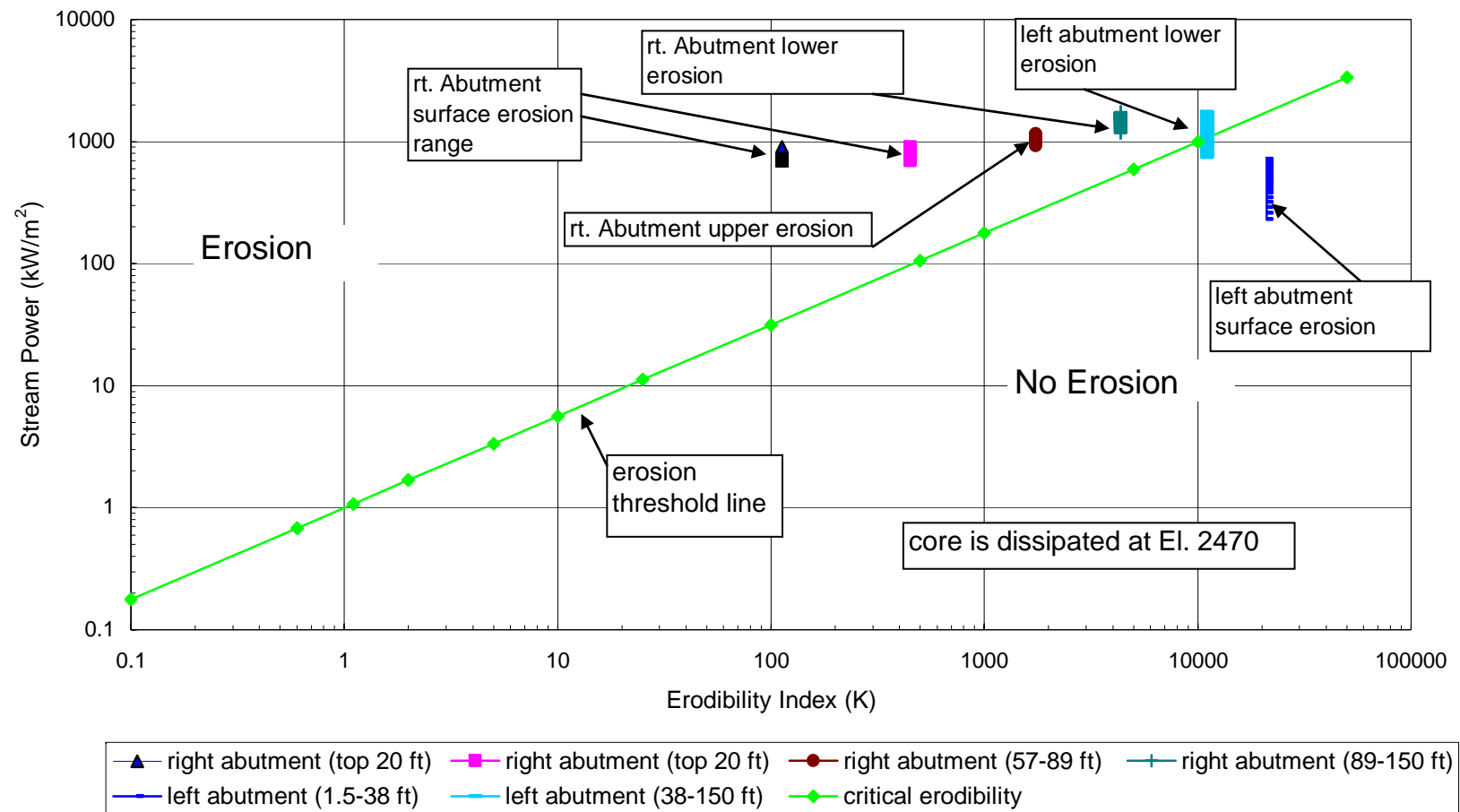


Figure 3A. - 50,000-year flood event. The core will dissipate at essentially the elevation of the tailwater.

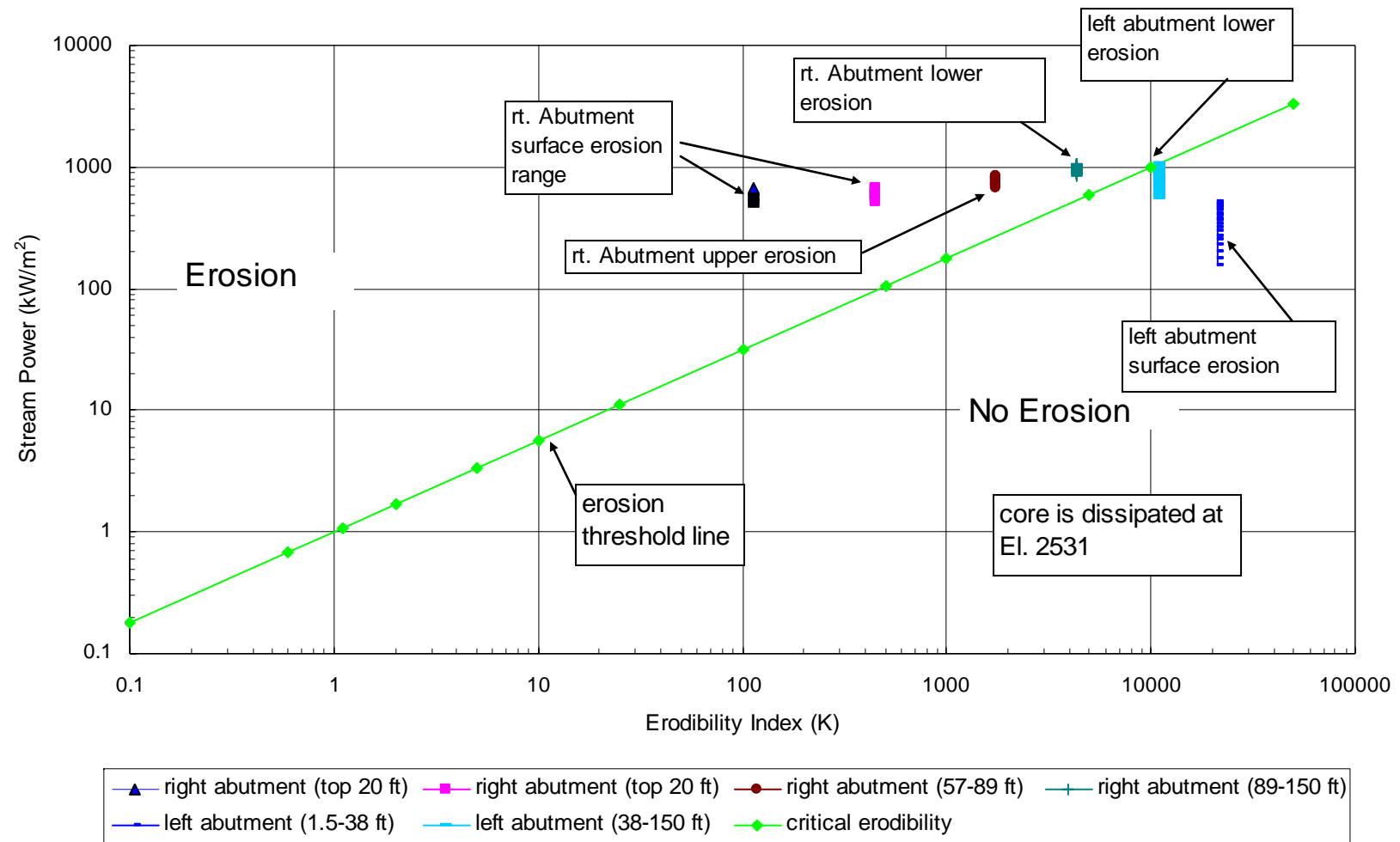


Figure 4A. - 20,000-year flood event. The core will dissipate at El. 2531 or about 30 ft above the tailwater.

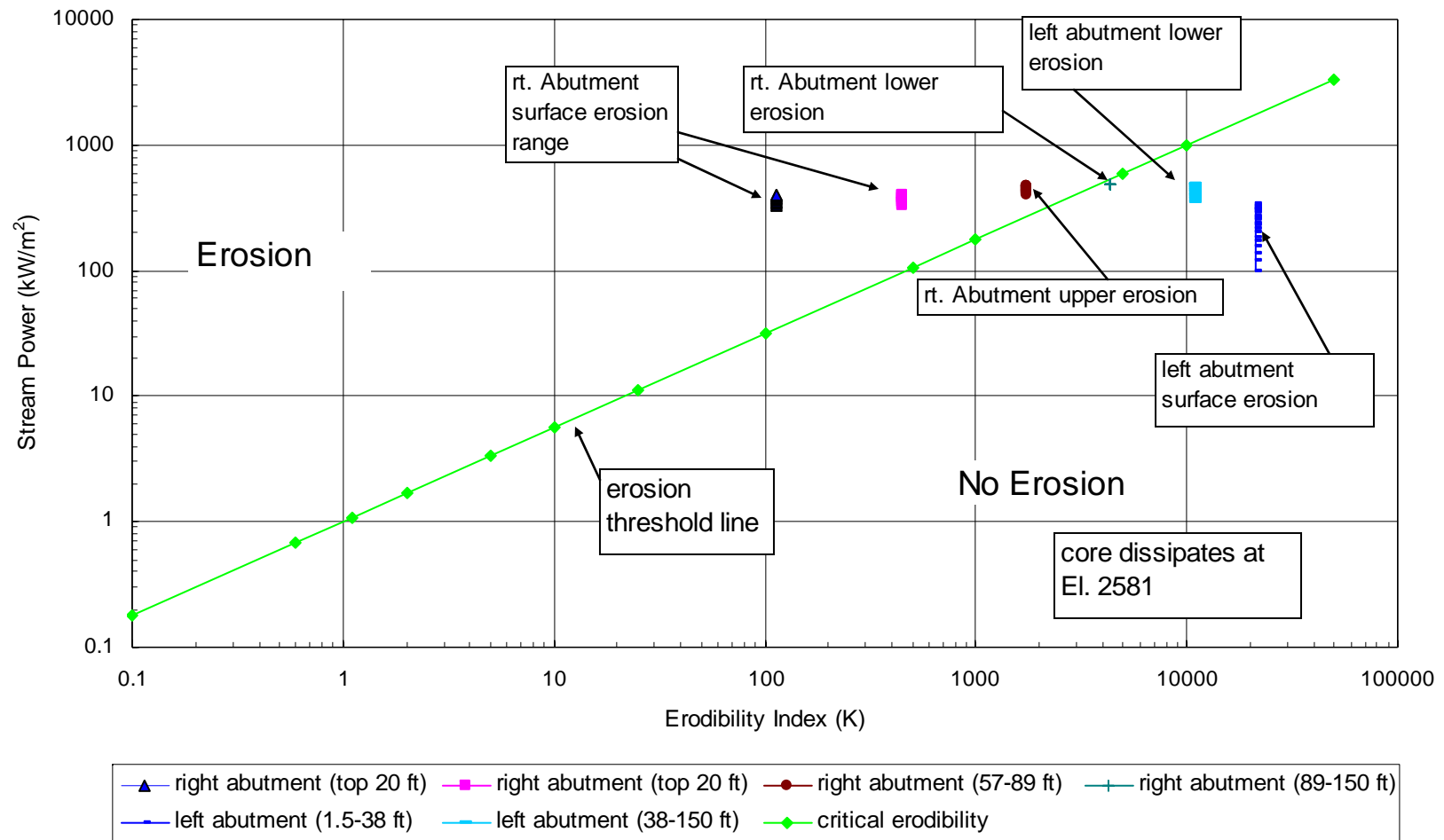


Figure 5A. - 10,000-year flood event. The core will dissipate at El. 2581 or about 30 feet above the tailwater.

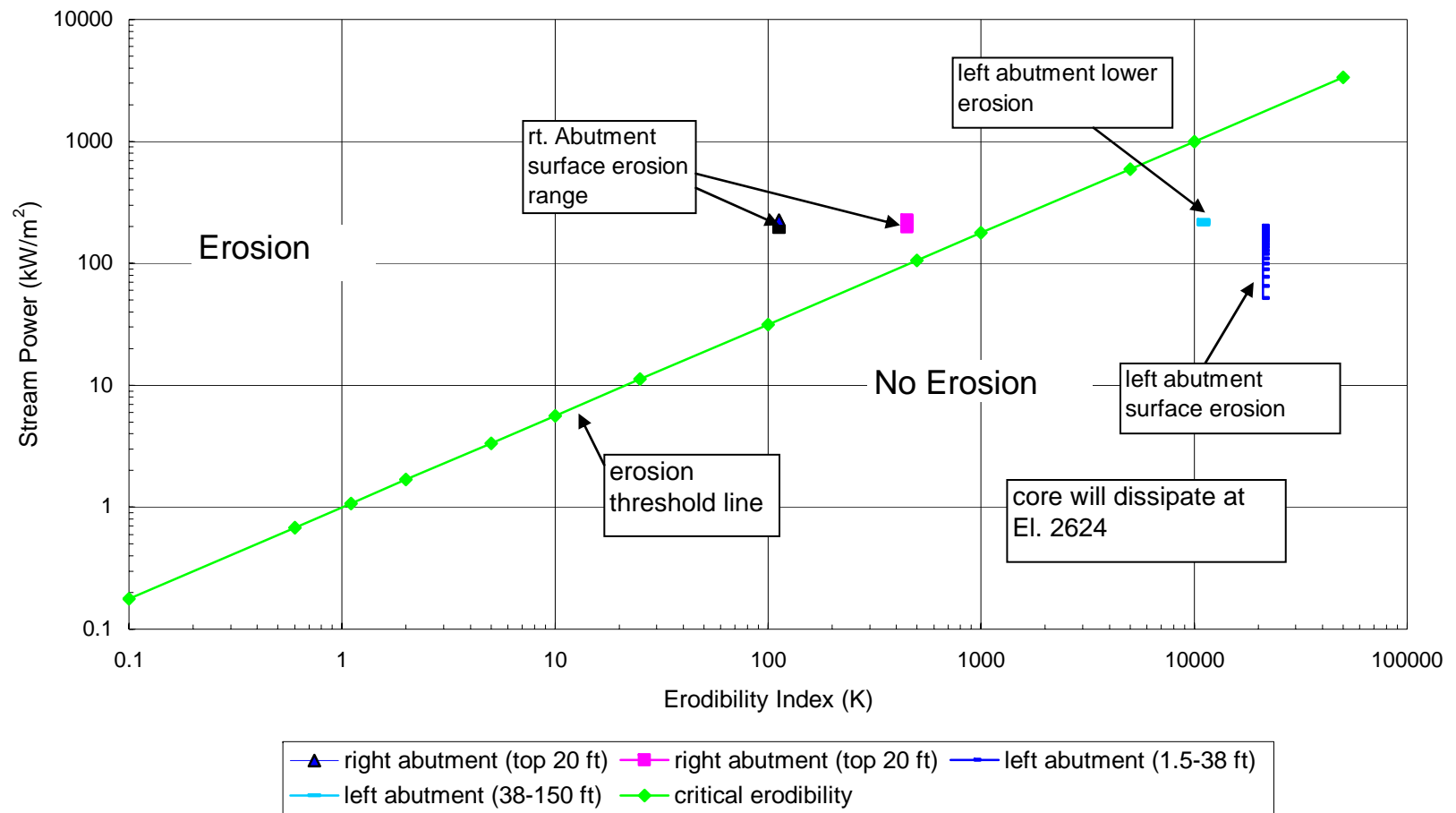


Figure 6A. - 5,000-year flood event. The core will dissipate about El. 2624 or 181 feet above the tailwater.